A non-cooperative decentralized model for Volt-VAr optimization of active distribution networks with multiple AC and DC microgrids

Author(s): Arpanahi, Moossa Khodadadi; Nateghi, Abolfazl; Heydarian-Forushani, Ehsan; Shafie-khah, Miadreza

Title: A non-cooperative decentralized model for Volt-VAr optimization of active distribution networks with multiple AC and DC microgrids

Year: 2023

Version: Accepted manuscript

Please cite the original version:

Arpanahi, M. K., Nateghi, A., Heydarian-Forushani, E. & Shafie-khah, M. (2023). A non-cooperative decentralized model for Volt-VAr optimization of active distribution networks with multiple AC and DC microgrids. *International Journal of Electrical Power & Energy Systems* 153, 109367. https://doi.org/10.1016/j.ijepes.2023.109367

A non-cooperative decentralized model for Volt-VAr optimization of active distribution networks with multiple AC and DC microgrids

Moossa Khodadadi Arpanahi [a,*], Abolfazl Nateghi [b], Ehsan Heydarian-Forushani [c], Miadreza Shafie-khah [d]

[a] Department of Electrical and Computer Engineering, Isfahan University of Technology (IUT), Isfahan, Iran

[b] Department of Electrical and Computer Engineering, Kharazmi University, Tehran, Iran

[c] Department of Electrical and Computer Engineering, Qom University of Technology, Qom, Iran

[d] Department of Technology and Innovations, University of Vaasa, Vaasa, Finland

Abstract

Volt-VAr optimization (VVO) is an important issue for distribution network operators in active distribution networks with a number of AC and DC microgrids. This paper introduces a coordinated decentralized framework with application to Volt-VAr optimization in distribution networks with multiple AC and DC microgrids in the presence of distributed energy resources (DERs). To this end, a non-cooperative coordination model is proposed so that micro-grids operators (MGOs) and distribution system operator (DSO) could minimize their own active power losses, separately. In fact, the DSO and MGOs interact together to achieve an equilibrium that satisfies their expected active power loss. In order to solve the proposed coordinated non-cooperative problem, a novel decentralized optimization approach is suggested so that the master problem is decomposed into two subproblems from DSO and MGOs point of views. These two sub-problems are linked to each other through sharing boundary information. On this basis, the communicational and computational loads are decreased while information secrecy is guaranteed. The modified IEEE 69-bus distribution network considering a number of AC and DC MGs has been chosen with the aim of conducting several numerical analyses.

1. Introduction

The microgrid includes a set of distributed energy resources (DERs) and loads located in a distribution network operating together which may operate in off-grid and grid-connected operation modes [1–3]. The microgrid plays a crucial role in future power grids according to its potential capabilities in various aspects such as reliability, security, resiliency, stability, and sustainability of power systems [4–7].

Integrating multiple microgrids (MMGs) is an appropriate method to enhance operation of microgrids and facilitate integration of DERs. Many researches have demonstrated benefits of integrating multiple microgrids in reliability enhancement [2], peer-to-peer energy trading [4], resilience improvement [3,5], real-time electricity market [6], increasing operational flexibility [7], optimal energy management [8–10], transactive energy [11–15], and voltage and frequency control [16–20]. A mixed integer linear programming (MILP) model for the networked microgrids including demand response (DR) and renewable energy sources (RESs) has been proposed in [8] using a scenario-based strategy for handling uncertainties and a novel pricing scheme for exchanging power among microgrids. Optimal energy management of MMGs has been studied in [9] introducing independency performance index (IPI) to decrease energy trading with the upstream network while voltage drop, system losses, and pollutant emissions have been also minimized. Reference [10] has proposed an energy management system (EMS) employing a cooperative game model in order to minimize operation cost of MMG coalitions including energy storage systems (ESSs), DR, and RESs in a 24-hour scheduling horizon. As a new concept for coordinating MMGs, transactive energy (TE) has been raised by some researchers in which microgrids independently participate in energy trading to reduce MMG system operation cost while satisfying the privacy and security of each sub-system. In this regard, a distributionally robust optimization TE framework has been suggested in [11] for energy scheduling among networked microgrids and upstream distribution network considering uncertainties of electricity price, RESs, demand, and electric vehicles (EVs). Modeling of transactive energy in MMG systems has been carried out using leader–follower game [12], hybrid competitive-cooperative game [14], and a decentralized framework

Nomenclature

Sets and Indices

$\mathbb{B}$, $\mathbb{L}$	Buses and lines sets
k, l, i	Buses, lines, and MGs indices

Parameters

$a^0_{k,l}$	1/-1 if bus k is sending/receiving node of line l; otherwise 0
$a^{\mathrm{I}}_{k,l}$	1 if node k is sending end of line l; otherwise 0
$a^{\mathrm{II}}_{k,l}$	1 if node k is receiving end of line l; otherwise 0
$\underline{\mathbb{V}}_k$, $\bar{\mathbb{V}}_k$	Lower and Upper limits for square of voltage of bus k
$\underline{P}^{ac}_k$, $\bar{P}^{ac}_k$	Lower and upper limits of active power exchange among DSO and AC MG at bus k
$\underline{Q}^{ac}_k$, $\bar{Q}^{ac}_k$	Lower and upper limits of reactive power exchange among DSO and AC MG at bus k
$\underline{P}^{dc}_k$, $\bar{P}^{dc}_k$	Lower and upper limits of active power exchange among DSO and DC MG at bus k
$\underline{P}^{up}_k$, $\bar{P}^{up}_k$	Lower and upper limits of reactive power exchange among DSO and transmission system at bus k
$\underline{P}^{up}_k$, $\bar{P}^{up}_k$	Lower and upper limits of reactive power exchange among DSO and transmission system at bus k
$\underline{Q}^{var}_k$, $\bar{Q}^{var}_k$	Lower and upper limits of reactive power of VAr compensator at bus k
$\bar{P}^{der}_k$	Upper limit for power generated by DER at bus k
$\bar{\mathbb{I}}_l$	Upper limit for square of current of line l
r_l x_l	Resistance and reactance of line l
P^{load}_k, Q^{load}_k	Active and reactive power load at bus k

Variables

P^{der}_k Q^{der}_k	Active and reactive power generation of DER at bus k
P^{gen}_k, Q^{gen}_k	Active and reactive power generation at bus k
P^{up}_k, Q^{up}_k	Active and reactive power exchange among DSO and transmission system at bus k
$P^{ex,ac}_k$, $Q^{ex,ac}_k$	Active and reactive exchange among DSO and AC MG at bus k
$P^{ex,dc}_k$	Amounts of active exchanged power among DSO and DC MG at bus k
P^{ls}_l, Q^{ls}_l	Active and reactive power loss of line l
Q^{var}_k	Reactive power of VAr compensator at bus k
P^{I}_l, Q^{I}_l	Active and reactive power of sending end of line l
P^{II}_l, Q^{II}_l	Active and reactive power of receiving end of line l
$\mathbb{V}_k$	Square of voltage of bus k
$\mathbb{I}_l$	Square of current of line l

according to alternating direction method of multipliers (ADMM) [15].

Among microgrids, interest on hybrid AC and DC microgrid is increasing due to the rapid increase in penetration of modern DC loads and DC power sources like photovoltaic (PV), fuel cell (FC), and ESSs, from one hand, and presence of existing AC power sources and loads from the other hand [21–23]. Hybrid AC and DC microgrid enjoys the benefits of both AC and DC microgrids and therefore it has been addressed in several researches in recent years which can be classified into two groups. One group has investigated control aspects of hybrid AC and DC microgrids and the other one has focused on the operation strategies, both in grid-connected and off-grid mode. Control schemes emphasis on the instantaneous operational conditions of voltage and frequency of the system [24–26] while the main objective of operation strategies is optimal hourly and sub-hourly operation of DERs [27]. Furthermore, optimal scheduling of hybrid AC and DC microgrids has been studied in [28].

The integration of AC and DC microgrids into distribution systems is one of the main solutions for increasing the benefits of DERs [29–31]. The AC and DC microgrids and distribution network are physically interconnected while operated independently. In fact, AC and DC microgrids are operated by microgrid managers (MGOs) whereas; distribution system is operated by distribution system operator (DSO). The coordination of DSO and MGOs can further increase the advantages of DERs for all sub-systems i.e. microgrids and distribution systems. Coordinated DSO-MGOs frameworks could be classified from various point of views. According to the literature review, the previously published papers generally concentrated on full cooperation method in that an performance indicator reflecting the whole system is optimized [32–34,36–39]. For instance, the authors in [33–35] have tried to minimize the total operation cost of existing MGOs and DSO.

Note that although the global optimum is obtained through full cooperation model, however, some players may not be satisfied and prefer to optimize their individual objectives, selfishly. On this basis, the current paper proposes a non-cooperative model for coordinated operation of DSO and MGOs so that each player could optimize its objective function independently.

In view of solution methodology, DSO and MGOs can be coordinated via centralized [34] or decentralized [33,35–38] manner. The centralized approach needs the collection of all gents' data in a control center, and the whole coordinated problem is solved through a controller unit, e.g. DSO or a third entity. However, the communicational and computational burdens of such centralization is high. In addition, DSO and MGOs are independent system operators and their privacy cannot be preserved using the centralized method. The deficits of centralized method have motivated researchers to propose decentralized solution methods such as Benders decomposition [33], ADMM [35], system of systems (SoS) approach [38], consensus method [39]. On the other hand, DSO and MGOs are coordinated for distinct operation, planning, and control problems [32–39]. In each problem, various techno-economic requirements are taken into account. To the best of authors' knowledge, the coordinated DSO-MGDs Volt-VAr optimization (VVO) has not been highlighted in the exiting researches in the area of DSO-MGOs coordination, especially when the both AC and DC microgrids are present.

VVO is one of the main problems both in distribution systems and microgrids which aims to determine optimal share of various reactive power sources such as synchronous DGs, renewables, and reactive power compensators in order to optimize an specific objective function while satisfying network constraints. Conventionally, distribution systems and microgrids solve their VVO problem in an independent way and without any coordination. Coordinated DSO-MGOs VVO is rarely investigated in the existing research work, especially by considering both AC and DC microgrids. On the other hand, other coordinated DSO-MGOs operation, control, or planning problems which are presented so far, mainly focus on the cooperative method as the approach for coordination of DSO and MGOs in which all system operators cooperate to minimize a desired objective function of whole system. Coordination of DSO and MGOs through a non-cooperative method in which agents tries to optimize their preferences selfishly studied in a few studies. This non-cooperative VVO method along with the studied cooperative method in the literature provides a better insight for system operators when they decide to solve their VVO problem in a coordinated way. Other main motivation of this paper is to develop a decentralized method for solving DSO-MGOs coordination problem. This motivation refers to the fact that the conventional centralized method in which all data are gathered in a central control and the problem is solved centrally is not consistent with the privacy of different independent system operators as they reluctant about disclosing their data. Besides, the problems pertaining to computational and communicational burden of centralization motivates the researchers to develop decentralized methods instead of coordinating problems in a centralized manner.

Motivated by the above-mentioned discussion, the current paper suggests a novel interactive decentralized model for coordination of DSO and MGOs within a distribution network including multiple AC and DC microgrids. In the proposed non-cooperative scheme, each system operator tends to selfishly solve its associated VVO problem, minimize the active power losses of its own network considering technical constraints of its network, and its associated active and (or) reactive power resources. The coordination is conducted based on a new decentralized method called partitioning and assignment of boundary Information (PABI) in which only information associated with boundary buses are shared. Thus, the suggested method ensures the privacy of each player. The proposed decentralized coordinated VVO framework can efficiently reduce power losses of each network so that all players are satisfied with their obtained solution. The equilibrium criteria of the decentralized non-cooperative method is determined based on Nash equilibrium concept. Therefore, proofs of essence and unity of the Nash equilibrium for the suggested DSO-MGOs coordinated scheme are also presented. To sum up, the contributions of this paper are summarized in below:

- To propose a non-cooperative model for coordinated operation of MGOs and DSO in an active distribution network including multiple AC and DC microgrids with the aim of VVO of either the AC or DC microgrids or also the distribution network, individually;
- To introduce a new decentralized method for integrating the sub-problems of MGOs and DSO in which boundary information are suitably split and assigned to DSO and the appropriate MGO. The employed approach could remarkably speed-up convergence of the decentralized scheme, diminish communication requirements, keep matching of boundary variables, and guarantee the privacy and independency of various players.

The rest of the paper is structured as follows. Section 2 deals with the mathematical modeling of the proposed decentralized non-cooperative loss minimization problem. The existence of Nash equilibrium and convergence of the proposed decentralized algorithm are presented in Section 3. The numerical results and analyses are given in Section 4. At end, section 5 assigns to conclusion.

2. Proposed decentralized non-cooperative Volt-VAr optimization scheme

In this section, a general description of the proposed decentralized non-cooperative VVO problem is presented. Moreover, the optimization problem from the viewpoint of existing players is formulated. Furthermore, the PABI decentralized method which is proposed for coordinating the interactions among the players is addressed. Finally, proofs of some theories associated with existence and singularity of equilibrium, and convergence of the suggested method are provided.

2.1. Conceptualization of the proposed method

According to Fig. 1, the paper assigns to a radial distribution network including a number of AC and DC microgrids. It is notable that there are a number of loads along with a number of generation units such as conventional and renewable-based DERs as well as reactive power sources such as capacitor banks (CBs) in each sub-network, i.e. microgrids and distribution network. The DC microgrids are also connected to the distribution network through AC/DC converters. The operator of distribution network is DSO, while the microgrids are operated by MGOs. A non-cooperative coordinated VVO model has been developed to efficiently minimize active power loss of existing microgrids and distribution network. In the proposed scheme, each player tries to

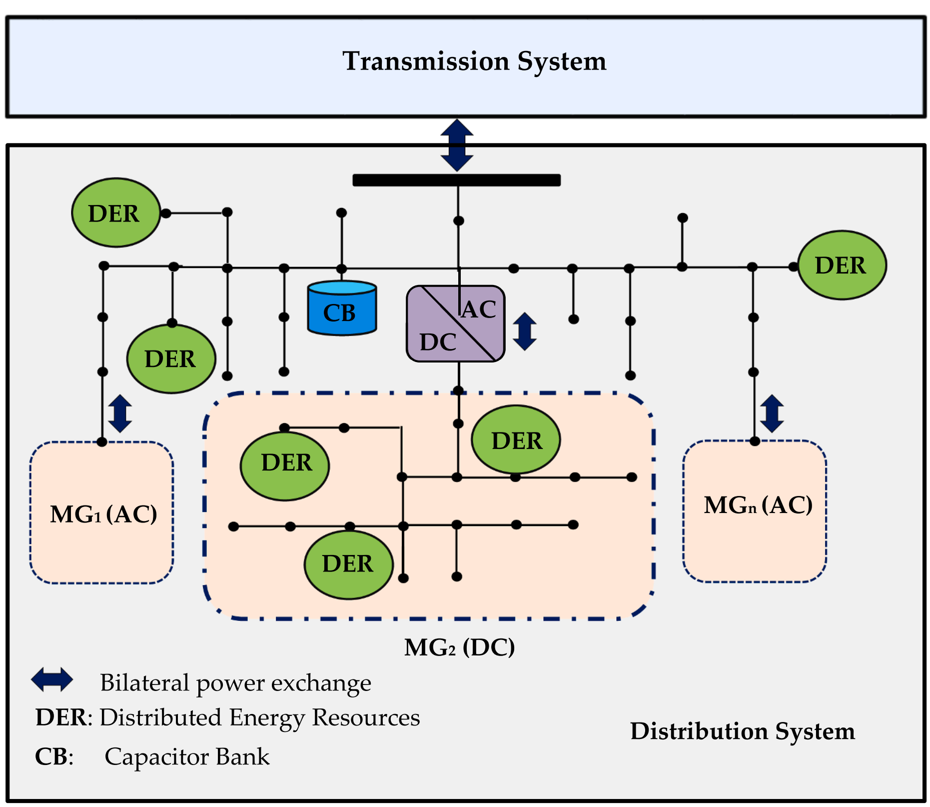

Fig. 1. Schematic of a typical distribution network with multiple AC and DC microgrids.

individually minimize the active power loss of its own network, while it has some interactions with other players through sharing boundary variables data. Therefore, the final solution could satisfy the objectives of all the players. In order to preserve the privacy of operators, a decentralized approach is used to solve the coordination problem. Before describing the coordination method, sub-problems of players, and decentralized solution approach, the following definitions are given.

Let $A = \{DSO, A_1, \cdots, A_a, D_1, \cdots, D_d\}$ be the set of players in which A_i and D_i are referred to AC and DC MGO_i, separately. The numbers of AC and DC microgrids are depicted through a and d, respectively. The strategy profile of the non-cooperative model is formulated as $\mathbb{S} = \prod_i \mathbb{S}_i = \mathbb{S}_{DSO} \times \mathbb{S}_{A_1} \times \cdots \times \mathbb{S}_{A_a} \times \mathbb{S}_{D_1} \times \cdots \times \mathbb{S}_{D_d}$ in which $\mathbb{S}_i$ represents strategy set of player i. According to Eq. (1), $\mathbb{S}_i$ is defined in terms of equality and inequality constraints of its slave problem where $\boldsymbol{u}_i$ is the strategy of player i.

$$\mathbb{S}_i = \{\boldsymbol{u}_i | h_i(\boldsymbol{u}_i) = 0\,,\; g_i(\boldsymbol{u}_i) \le 0\} \tag{1}$$

The player i optimizes its utility function $\mathcal{U}_i$ that is formulated for DSO and every MGO through Eq. (2).

$$\mathcal{U}_{DSO} = -f_{DSO}(\boldsymbol{u}) \tag{2a}$$

$$\mathcal{U}_{A_i} = -f_{A_i}(\boldsymbol{u}) \quad \forall i = 1, 2, \cdots, a \tag{2b}$$

$$\mathcal{U}_{D_i} = -f_{D_i}(\boldsymbol{u}) \quad \forall i = 1, 2, \cdots, d \tag{2c}$$

where f_{DSO}, f_{A_i}, and f_{D_i} are the objective functions of DSO, AC MGO_i and DC MGO_i, respectively. Based on Eq. (2), the objective function of each player depends on decisions made by the other players, i.e. $\boldsymbol{u} = \{\boldsymbol{u}_{DSO}, \boldsymbol{u}_{A_1}, \cdots, \boldsymbol{u}_{A_a}, \boldsymbol{u}_{D_1}, \cdots, \boldsymbol{u}_{D_d}\}$. In the next sub-section, sub-problems of players are described.

2.2. Sub-problems of players

The formulations associated with the sub-problems of DSO and AC and DC microgrids are given in this sub-section.

2.2.1. Objective functions

As formulated in (3), the players including DSO and AC/DG MGOs try to minimize active power loss of their own network, respectively.

$$\text{DSO}: \;\; \text{Min}\; f_{DSO} = \sum_{l \in \mathbb{L}_{DSO}} P_l^{ls} \tag{3a}$$

$$\text{AC MGO}\, i: \;\; \text{Min}\; f_{A_i} = \sum_{l \in \mathbb{L}_{A_i}} P_l^{ls} \tag{3b}$$

$$\text{DC MGO}\, i: \;\; \text{Min}\; f_{D_i} = \sum_{l \in \mathbb{L}_{D_i}} P_l^{ls} \tag{3c}$$

In fact, each player tends to individually optimize active power losses of its own grid while satisfying the relevant constraints of its network and resources close to real-time period e.g. a fragment of an hour. Decision variables of players are given by Eq. (4), where k and l are indices of buses and lines of the network.

$$\boldsymbol{u}_{D_i} = [P_k^{der}, P_k^{ex,dc}, P_l^{\text{I}}, P_l^{\text{II}}, P_l^{ls}, \mathbb{V}_k, \mathbb{I}_l] \tag{4a}$$

$$\boldsymbol{u}_{A_i} = [P_k^{der}, P_k^{ex,ac}, P_l^{\text{I}}, P_l^{\text{II}}, P_l^{ls}, Q_k^{der}, Q_k^{var}, Q_k^{ex,ac}, Q_l^{\text{I}}, Q_l^{\text{II}}, Q_l^{ls}, \mathbb{V}_k, \mathbb{I}_l] \tag{4b}$$

$$\boldsymbol{u}_{DSO} = [P_k^{der}, P_k^{up}, P_k^{ex,dc}, P_l^{\text{I}}, P_l^{\text{II}}, P_l^{ls}, Q_k^{der}, Q_k^{up}, Q_k^{var}, Q_k^{ex,ac}, Q_l^{\text{I}}, Q_l^{\text{II}}, Q_l^{ls}, \mathbb{V}_k, \mathbb{I}_l] \tag{4c}$$

According to (4a), decision variables of DC MGO i are active powers of DERs, P_k^{der}, active power exchange between DSO and DC MGO i, $P_k^{ex,dc}$, active power of sending and reconvening ends of lines, $P_l^{\text{I}}/P_l^{\text{II}}$, and active power losses of the lines, P_l^{ls}. Furthermore, square of voltage magnitude, $\mathbb{V}_k$, and square of current magnitude, $\mathbb{I}_k$, are determined.

As (4b) shows, in sub-problem of AC MGO i, in addition to active powers, $Q_k^{der}, Q_k^{var}, Q_k^{ex,ac}, Q_l^{\text{I}}, Q_l^{\text{II}}$, and Q_l^{ls} are also determined which are reactive powers of DERs, reactive powers of VAr compensators, reactive power exchange between DSO and AC MGO i, reactive power of sending and reconvening ends of lines, and reactive power losses of the lines. Decision variables of DSO sub-problem is same as sub-problem of AC MGOs, however, active/reactive exchanged power among both AC and DC microgrids are presented in sub-problem of DSO.

2.2.2. The constraints related to sub-problems of DSO and AC MGOs

Equations (5) and (6) ensure balance of active and reactive power at each bus. The Kirchhoff's voltage law in line l has been modeled based on the second-order cone relaxation (SOCR) through Eq. (7) and Eq. (8). The formulation related to active power loss of line l is given in Eq. (9) by means of square of current magnitude as well as sending and receiving nodes. The formulation associated with reactive power loss of line l due to its active power loss as well as reactive powers at send and receive nodes is given in Eq. (10). The allowable ranges of voltage and current magnitudes are illustrated in Eq. (11). The power generated by DGs are restricted through Eq. (12) and Eq. (13), where $\mathfrak{a}_k$, $\mathfrak{b}_k$, α_k, β_k, and $\widetilde{Q}_k^{der}$ are pre-defined parameters [39]. Equations (12) and (13) describe the operational region of DERs based on reactive power capability curve of Fig. 2. The value of these parameters could specify the DG technology including renewable-based or conventional DGs. Equation (14) restricts the reactive power of VAr compensators. The transacted active/reactive power among distribution network and AC microgrids is restricted through Eq. (15). Moreover, the power exchange among distribution network and transmission network must not exceed than a pre-specified value according to Eq. (16). The constraints related to AC/DC converters have been also considered based on [31]. It is noteworthy that the coefficients $a_{k,l}^0$, $a_{k,l}^I$, and $a_{k,l}^{II}$ are related to the network connection matrixes.

$\forall k \in \mathbb{B}, l \in \mathbb{L}:$

$$P_k^{gen} = P_k^{load} + \sum_l a_{k,l}^{\text{I}} P_l^{\text{I}} - \sum_l a_{k,l}^{\text{II}} P_l^{\text{II}} \tag{5a}$$

$$P_k^{gen} = P_k^{der} + P_k^{up} + P_k^{ex,ac} + P_k^{ex,dc} \tag{5b}$$

$$Q_k^{gen} = Q_k^{load} + \sum_l a_{k,l}^{\text{I}} Q_l^{\text{I}} - \sum_l a_{k,l}^{\text{II}} Q_l^{\text{II}} \tag{6a}$$

$$Q_k^{gen} = Q_k^{der} + Q_k^{var} + Q_k^{up} + Q_k^{ex,ac} \tag{6b}$$

$$\sum_{k \in \mathbb{B}} a_{k,l}^0 \mathbb{V}_k = r_l(P_l^{\text{I}} + P_l^{\text{II}}) + x_l(Q_l^{\text{I}} + Q_l^{\text{II}}) \tag{7}$$

$$\left\| \begin{matrix} 2P_l^{\text{I}} \\ 2Q_l^{\text{I}} \\ \mathbb{I}_l - \sum_{k \in \mathbb{B}} a_{k,l}^{\text{I}} \mathbb{V}_i \end{matrix} \right\|_2 \le \mathbb{I}_l + \sum_{k \in \mathbb{B}} a_{k,l}^{\text{I}} \mathbb{V}_k \tag{8}$$

$$P_l^{ls} = r_l \mathbb{I}_l = P_l^{\text{I}} - P_l^{\text{II}} \tag{9}$$

$$Q_l^{ls} = (x_l/r_l) P_l^{ls} = Q_l^{\text{I}} - Q_l^{\text{II}} \tag{10}$$

$$\underline{\mathbb{V}}_k \le \mathbb{V}_k \le \bar{\mathbb{V}}_k,\; \mathbb{I}_l \le \bar{\mathbb{I}}_l \tag{11}$$

$$-\mathfrak{a}_k P_k^{der} \le Q_k^{der} \le \mathfrak{b}_k P_k^{der},\; P_k^{der} \le \overline{P}_k^{der} \tag{12}$$

$$-\widetilde{Q}_k^{der} + \beta_k\left(P_k^{der} - \overline{P}_k^{der}\right) \le Q_k^{der} \le \widetilde{Q}_k^{der} - \alpha_k(P_k^{der} - \overline{P}_k^{der}) \tag{13}$$

$$\underline{Q}_k^{var} \le Q_k^{var} \le \overline{Q}_k^{var} \tag{14}$$

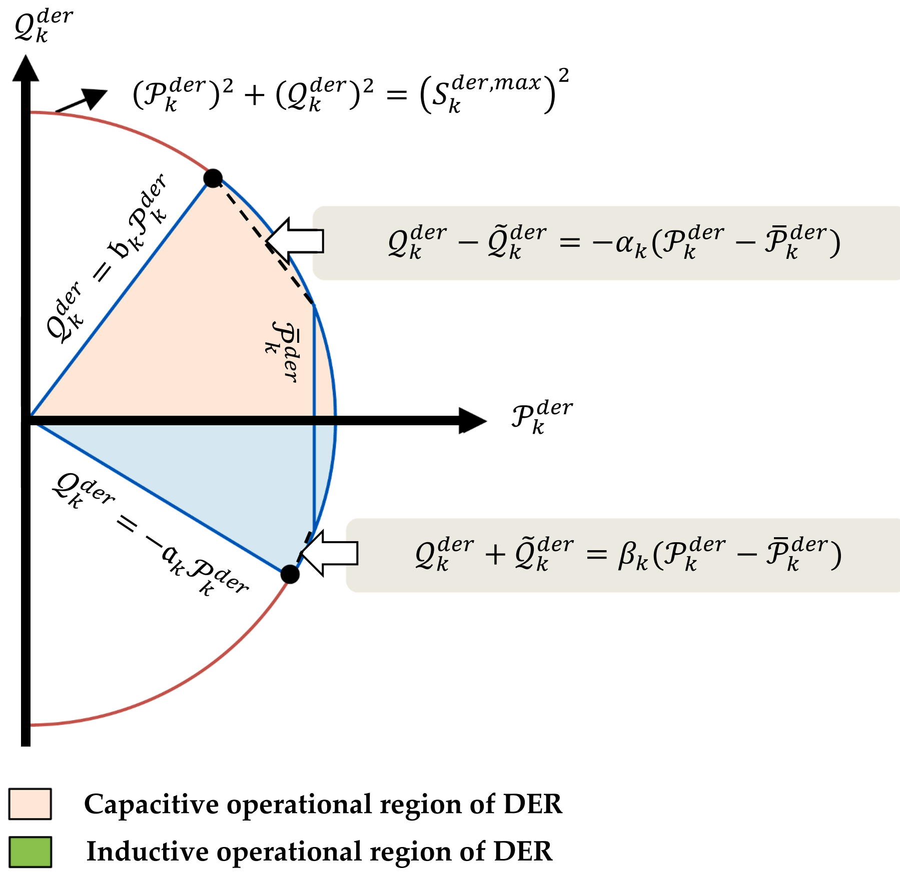

Fig. 2. Reactive power capability curve of DERs.

$$\underline{P}_k^{ac} \leq P_k^{ex,ac} \leq \overline{P}_k^{ac},\ \underline{Q}_k^{ac} \leq Q_k^{ex,ac} \leq \overline{Q}_k^{ac} \tag{15}$$

$$\underline{P}_k^{up} \leq P_k^{up} \leq \overline{P}_k^{up},\ \underline{Q}_k^{up} \leq Q_k^{up} \leq \overline{Q}_k^{up} \tag{16}$$

2.2.3. *The constraints related to Sub-Problems of DC MGOs*

The constraints of (5), (9), and (10) must be reconsidered for DC microgrids. Also, the Kirchhoff's voltage law according to SOCR format is formulated through Eq. (17) and (18) for line l. The restrictions regarding active power output of DERs have been modeled in Eq. (19). The transacted power among distribution network and DC microgrids is restricted through Eq. (20).

$\forall k \in \mathbb{B}, l \in \mathbb{L}:$

$$\sum_{k\in\mathbb{B}} a_{k,l}^0 \mathbb{V}_k = r_l(P_l^{\mathrm{I}} + P_l^{\mathrm{II}}) \tag{17}$$

$$\left\| \begin{matrix} 2P_l^{\mathrm{I}} \\ \mathbb{I}_l - \sum_{k\in\mathbb{B}} a_{k,l}^{\mathrm{I}} \mathbb{V}_k \end{matrix} \right\|_2 \leq \mathbb{I}_l + \sum_{k\in\mathbb{B}} a_{k,l}^{\mathrm{I}} \mathbb{V}_k \tag{18}$$

$$0 \leq P_k^{der} \leq \overline{P}_k^{der} \tag{19}$$

$$\underline{P}_k^{dc} \leq P_k^{ex,dc} \leq \overline{P}_k^{dc} \tag{20}$$

2.3. *Solve the non-cooperative coordinated problem through the proposed decentralized method*

This sub-section assigns to describe the proposed decentralized method with the aim of solving the DSO-MGOs coordinated VVO scheme. The proposed decentralized method so-called PABI is described in below:

First, according to (21), the decision variables of the proposed coordinated problem are split into four categories.

$$\boldsymbol{u} = \{\boldsymbol{u}_{ind}^{DSO} \bigcup \boldsymbol{u}_{ind}^{A} \bigcup \boldsymbol{u}_{ind}^{D} \bigcup \boldsymbol{u}_B\} \tag{21}$$

where the decision variables $\boldsymbol{u}_{ind}^{DSO}$ are only related to DSO and are called DSO's individual decision variables because these variables are decided only by DSO. Also, $\boldsymbol{u}_{ind}^{A}$ represents the decision variables associated with the AC microgrids which is defined in Eq. (22). Note that, $\boldsymbol{u}_{ind}^{A_i}$ represents the decision variables of AC microgrid i ($\forall i = 1, 2, \cdots, a$). Likewise, $\boldsymbol{u}_{ind}^{D}$ indicates the decision variable's set of DC microgrids and according to (22) can be represented in terms of individual decision variables of DC microgrid i, i.e. $\boldsymbol{u}_{ind}^{D_i}$ ($\forall i = 1, 2, \cdots, d$).

$$\boldsymbol{u}_{ind}^{A} = \begin{bmatrix} \boldsymbol{u}_{ind}^{A_1} \\ \vdots \\ \boldsymbol{u}_{ind}^{A_a} \end{bmatrix},\ \boldsymbol{u}_{ind}^{D} = \begin{bmatrix} \boldsymbol{u}_{ind}^{D_1} \\ \vdots \\ \boldsymbol{u}_{ind}^{D_d} \end{bmatrix} \tag{22}$$

The set of boundary variables in (21), $\boldsymbol{u}_B$, is expressed in Eq. (23).

$$\boldsymbol{u}_B = [\boldsymbol{u}_{B_1} \quad \cdots \quad \boldsymbol{u}_{B_a} \ \boldsymbol{u}_{B_{a+1}} \quad \cdots \quad \boldsymbol{u}_{B_{a+d}}] \tag{23}$$

where $\boldsymbol{u}_{B_i}$ is the set of boundary variables at boundary i ($\forall i = 1, 2, \cdots, a + d$). In this paper, the PABI approach is used to define the transactions among AC and DC microgrids and DSO as illustrated in Fig. 3. Due to the PABI methodology, boundary variables related to the boundary bus of AC microgrid i and the distribution network are defined through Eq. (24).

$$\boldsymbol{u}_{B_i} = \boldsymbol{u}_{B_i}^{DSO} \cup \boldsymbol{u}_{B_i}^{A_i} \quad 1 \leq i \leq a \tag{24}$$

Similarly, Eq. (25) formulates the boundary variables of the

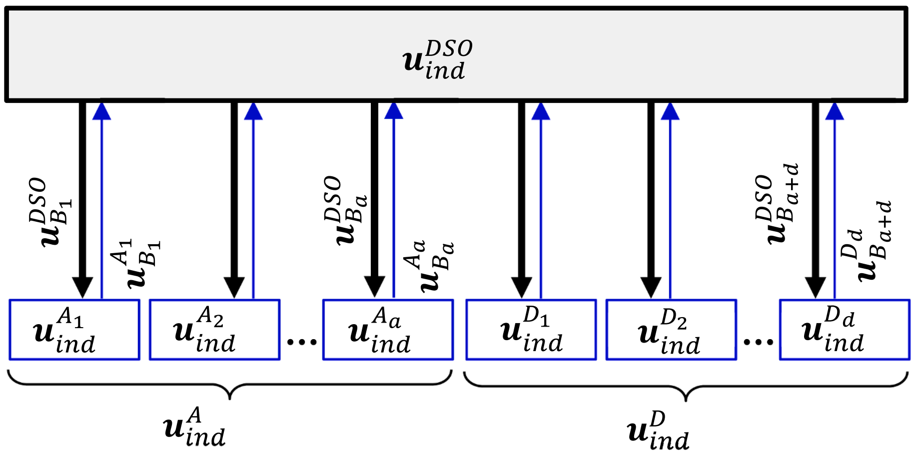

Fig. 3. PABI technique.

distribution network and DC microgrid i.

$$\boldsymbol{u}_{B_i} = \boldsymbol{u}_{B_i}^{DSO} \cup \boldsymbol{u}_{B_i}^{D_{i-a}} \quad a+1 \le i \le a+d \tag{25}$$

According to (24) and (25), the boundary bus among two connected systems such as distribution network and an AC or DC microgrid, has several boundary variables that can be partitioned into two groups. The first group, $\boldsymbol{u}_{B_i}^{DSO}$, pertains to DSO decision variables. Thus, the DSO could determine these boundary variables. Whenever DSO makes decision regarding its own sub-problem, its associated decision variables are obtained and also shared with the relevant AC and DC MGOs. As Fig. 3 shows, the second group of boundary variables at boundary i is $\boldsymbol{u}_{B_i}^{A_i}$ ($\boldsymbol{u}_{B_i}^{D_{i-a}}$) and it is assigned to AC MGO_i (DC MGO_i). Once AC MGO_i (DC MGO_i) solves its own sub-problem, it could obtain $\boldsymbol{u}_{B_i}^{A_i}$ ($\boldsymbol{u}_{B_i}^{D_{i-a}}$) and share the calculated values with DSO. This interactive procedure continues until the convergence of the whole coordinated problem.

The consistency constraints must be included in order to guarantee matching of boundary variables in the related sub-problems in the decentralized optimization methods such as ADMM. These constraints must be satisfied in order to ensure convergence of the decentralized algorithm. In general, the boundary variables are calculated by all involved players so that each player tries to follow the boundary variables obtained by other players. Matching boundary variables in such a way could increase the iterations and subsequently the calculation time. To solve the mention challenge, this article exploits PABI technique to match boundary variables. As described earlier, this method removes the need to directly insert the consistency constraints in sub-problems. In fact, the boundary variables of each boundary are categorized into two sets. Each set of boundary variables is calculated by one decision-maker and shared with others. Therefore, in each iteration, sub-problems of two neighboring sub-systems use a same amount for a particular boundary decision variable. Because of this feature, the convergence speed of the proposed interactive decentralized method is substantially increased compared to other decentralized methods. Furthermore, the proposed decentralized method does not require the any setting for the parameters. Moreover, the number of shared variables among DSO and MGOs is decreased that may result in communication burden reduction between DSO and MGOs.

The active/reactive exchanged powers, voltage phase and amplitude at the boundary bus are the boundary variables of the distribution network and AC microgrids. The following rule is established based on the PABI approach. The DSO optimizes its own sub-problem for pre-specified amounts of active and reactive power and then, calculates the magnitude and phase of boundary voltages. Afterward, the obtained boundary voltages are shared with MGOs so that they could optimize their own sub-problems through the shared data and hence, the amounts of active and reactive power exchanges are updated. This procedure is continued as long as convergence is achieved for all the boundary variables. Note that the mechanism is completely similar for interaction among DSO and each DC MGO except that the voltage and active power are the boundary variables in this case. The boundary bus voltage is determined by DSO, while the active exchanged power is calculated through DC MGO. Afterward, the obtained values are shared. The sub-problems associate with each player can be written based on the proposed PABI method as it can be observed in Eqs. (26)-(28).

$$\begin{aligned}
&\text{DSO: } \textit{Minimize } f_{DSO}\left(\boldsymbol{u}_{ind}^{DSO}, \boldsymbol{u}_{B_1}^{DSO}, \cdots, \boldsymbol{u}_{B_{a+d}}^{DSO}, \bar{\boldsymbol{u}}_{B_1}^{A_1}, \cdots, \bar{\boldsymbol{u}}_{B_{a+d}}^{D_d}\right)\\
&g_{DSO}\left(\boldsymbol{u}_{ind}^{DSO}, \boldsymbol{u}_{B_1}^{DSO}, \cdots, \boldsymbol{u}_{B_{a+d}}^{DSO}, \bar{\boldsymbol{u}}_{B_1}^{A_1}, \cdots, \bar{\boldsymbol{u}}_{B_{a+d}}^{D_d}\right) \le 0\\
&h_{DSO}\left(\boldsymbol{u}_{ind}^{DSO}, \boldsymbol{u}_{B_1}^{DSO}, \cdots, \boldsymbol{u}_{B_{a+d}}^{DSO}, \bar{\boldsymbol{u}}_{B_1}^{A_1}, \cdots, \bar{\boldsymbol{u}}_{B_{a+d}}^{D_d}\right) = 0
\end{aligned} \tag{26}$$

$$\begin{aligned}
&\text{AC MGO } i: \textit{Minimize } f_{A_i}(\boldsymbol{u}_{ind}^{A_i}, \boldsymbol{u}_{B_i}^{A_i}, \bar{\boldsymbol{u}}_{B_i}^{DSO})\\
&g_{A_i}(\boldsymbol{u}_{ind}^{A_i}, \boldsymbol{u}_{B_i}^{A_i}, \bar{\boldsymbol{u}}_{B_i}^{DSO}) \le 0\\
&h_{A_i}(\boldsymbol{u}_{ind}^{A_i}, \boldsymbol{u}_{B_i}^{A_i}, \bar{\boldsymbol{u}}_{B_i}^{DSO}) = 0\\
&\forall i = 1, 2, \cdots, a
\end{aligned} \tag{27}$$

$$\begin{aligned}
&\text{DC MGO } i: \textit{Minimize } f_{D_i}(\boldsymbol{u}_{ind}^{D_i}, \boldsymbol{u}_{B_{i+a}}^{D_i}, \bar{\boldsymbol{u}}_{B_{i+a}}^{DSO})\\
&g_{D_i}(\boldsymbol{u}_{ind}^{D_i}, \boldsymbol{u}_{B_i}^{D_i}, \bar{\boldsymbol{u}}_{B_i}^{DSO}) \le 0\\
&h_{D_i}(\boldsymbol{u}_{ind}^{D_i}, \boldsymbol{u}_{B_i}^{D_i}, \bar{\boldsymbol{u}}_{B_i}^{DSO}) = 0\\
&\forall i = 1, \cdots, d
\end{aligned} \tag{28}$$

In (26), f_{DSO}, g_{DSO}, and h_{DSO} represents objective function, non-equality constraints, and equality constraints of DSO sub-problem and are generally functions of individual and assigned boundary variables of DSO. It should be noted that, the sign '$\bar{\ }$' means that boundary variables assigned to AC and DC MGOs are known in DSO sub-problem because DSO receives these variables from AC and DC MGOs. Likewise, the functions f_{A_i}, g_{A_i}, and h_{A_i} in (27) indicate objective function, non-equality constraints, and equality constraints of AC MGO i. These functions depends on AC MGO i individual variables, $\boldsymbol{u}_{ind}^{A_i}$, and boundary variables of distribution network-AC microgrid i boundary bus that are assigned to AC MGO i, i.e. $\boldsymbol{u}_{B_i}^{A_i}$. As (27) demonstrates among distribution network-AC microgrid i boundary variables, $\bar{\boldsymbol{u}}_{B_i}^{DSO}$ are kept constant in sub-problem of AC MGO i. Equation (28) can be similarly explained for DC MGO.

The proposed non-cooperative scheme seeks for finding the Nash equilibrium solution $\boldsymbol{u}^\star$ i.e. the solution that no player could reach a better value for its utility function as shown mathematically in Eq. (29).

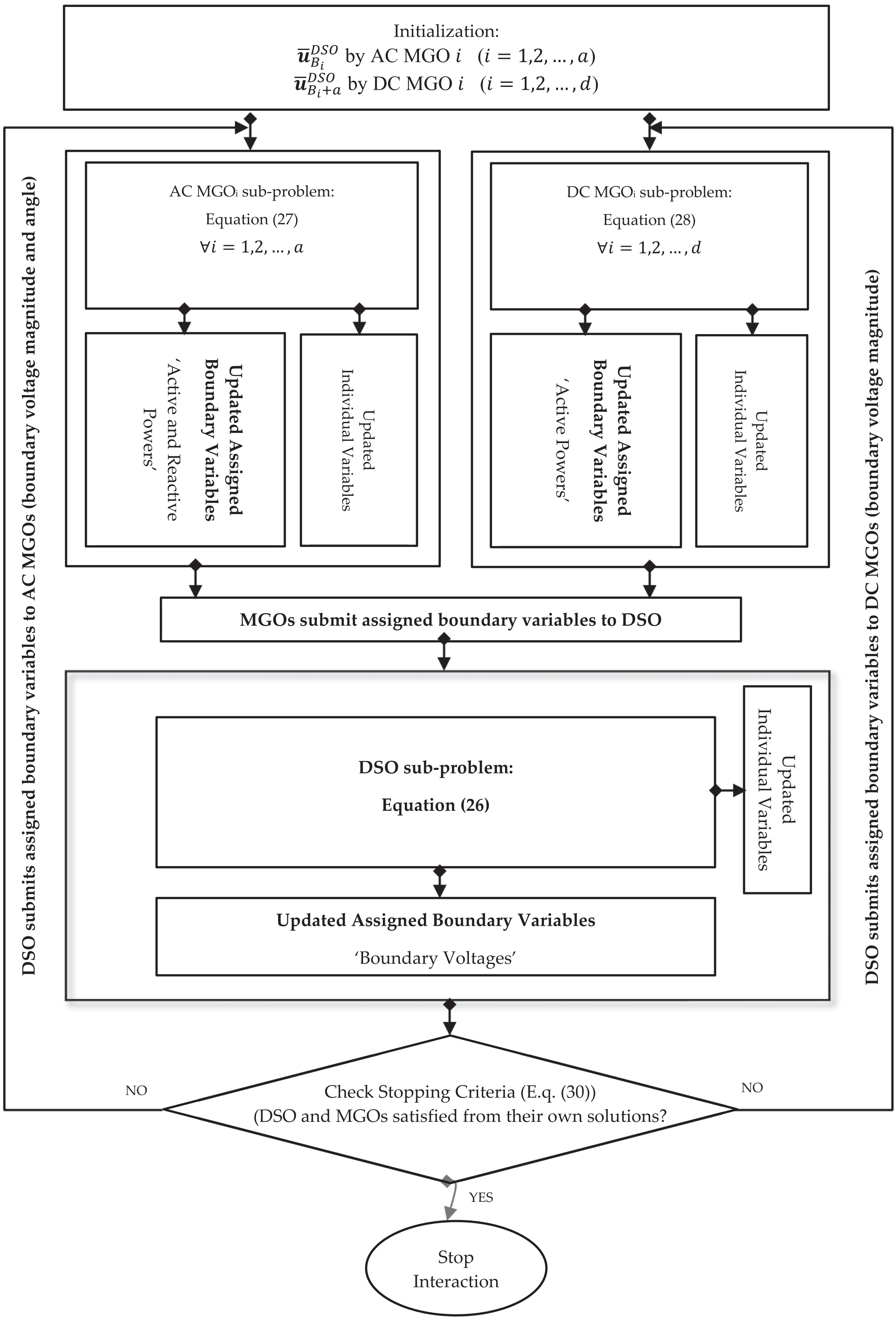

Fig. 4. The flowchart of the proposed decentralized scheme.

$$\mathscr{U}_{DSO}(\boldsymbol{u}^\star) \geq \mathscr{U}_{DSO}(\boldsymbol{u}_{DSO}, \boldsymbol{u}^\star_{A_1}, \cdots, \boldsymbol{u}^\star_{A_a}, \boldsymbol{u}^\star_{D_1}, \cdots, \boldsymbol{u}^\star_{D_d})$$
$$\mathscr{U}_{A_i}(\boldsymbol{u}^\star) \geq \mathscr{U}_{A_i}\left(\boldsymbol{u}^\star_{DSO}, \boldsymbol{u}^\star_{A_1}, \cdots, \boldsymbol{u}_{A_i}, \cdots, \boldsymbol{u}^\star_{A_a}, \boldsymbol{u}^\star_{D_1}, \cdots, \boldsymbol{u}^\star_{D_d}\right)$$
$$\forall i = 1, 2, \cdots, a \tag{29}$$
$$\mathscr{U}_{D_i}(\boldsymbol{u}^\star) \geq \mathscr{U}_{D_i}\left(\boldsymbol{u}^\star_{DSO}, \boldsymbol{u}^\star_{A_1}, \cdots, \boldsymbol{u}^\star_{A_a}, \boldsymbol{u}^\star_{D_1}, \cdots, \boldsymbol{u}_{D_i}, \cdots, \boldsymbol{u}^\star_{D_d}\right)$$
$$\forall i = 1, \cdots, d$$

To solve the proposed non-cooperative coordinated scheme in a decentralized approach through the PABI method and Nash equilibrium concept, an iterative algorithm is used as shown in Fig. 4. Without loss of generality, it is assumed that MGOs starts the algorithm. For this purpose, AC and DC MGOs select initial values for boundary variables assigned to DSO i.e. $\bar{\boldsymbol{u}}^{DSO}_{B_i}$ ($\forall i = 1, \cdots a, \cdots, a + d$). Then, all MGOs parallelly run their sub-problems using (27) and (28) and obtain updated values for their individual and assigned boundary variables. Each MGO sends its assigned boundary variables to DSO. In the next stage, once DSO receives $\left[\boldsymbol{u}^{A_1}_{B_1} \quad \cdots \quad \boldsymbol{u}^{A_a}_{B_a} \quad \boldsymbol{u}^{D_1}_{B_{a+1}} \quad \cdots \quad \boldsymbol{u}^{D_d}_{B_{a+d}}\right]$ that is the set of boundary variables assigned to MGOs, it solves its sub-problem according to (26). Finally, the algorithm checks the stopping criteria expressed by (30) and decides on the termination or continuation of the process. According to Eq. (30), in iteration k, if objective function of each sufficiently approaches to its value in iteration $(k-1)$, i.e. each objective function is optimized for the particular solution of the other players in order to obtain the Nash equilibrium and then, the algorithm is stopped. Otherwise, DSO submits the updated values obtained for its assigned boundary variables $\boldsymbol{u}^{DSO}_{B_i}$ ($\forall i$) to MGOs so that they can resolve their sub-problem.

$$\left|f^{(k)}_{DSO} - f^{(k-1)}_{DSO}\right| \leq \mathscr{E}_{DSO} \tag{30a}$$

$$\left|f^{(k)}_{A_i} - f^{(k-1)}_{A_i}\right| \leq \mathscr{E}_{A_i} \tag{30b}$$

$$\left|f^{(k)}_{D_i} - f^{(k-1)}_{D_i}\right| \leq \mathscr{E}_{D_i} \tag{30c}$$

In Eq. (30), $f^{(k)}_{DSO}, f^{(k)}_{A_i}$, and $f^{(k)}_{D_i}$ are the values assigned to the objective functions of DSO, AC MG_i, and DC MG_i in iteration k, separately. Also, $\mathscr{E}_{DSO}$, $\mathscr{E}_{A_i}$, and $\mathscr{E}_{D_i}$ are pre-determined small thresholds.

An important point about Fig. 4 that should be noted is that, in the proposed method, the boundary variables at each boundary have been partitioned into two groups. The first set of boundary variables is assigned to MGs while the second set is associated with DSO. The boundary variables among AC MGs and distribution network are active power (P), reactive power (Q), magnitude (V), and angle (θ) of boundary voltage where PQ have been assigned to AC MG operators, while Vθ are associated with the distribution network operator. It is noteworthy that, the boundary variables among DC MGs and distribution network are P and V so that P and V are assigned to DC MG operators and distribution network operator, respectively. For more clarification, in each iteration the AC MGs solve their own objective functions and calculate optimal P and Q and share it with DSO. Afterward, the DSO calculates V and θ taking into account P and Q values and shares the results with AC MGs. The aforementioned procedure will be continued until achieving convergence. According to what mentioned in this subsection, the indicator for evaluating Nash equilibrium is convergence of objective functions (30) that means that all agents are satisfied with their solution and the equilibrium is obtained.

3. Proofs of some theories

The existence of Nash equilibrium and convergence of the proposed decentralized algorithm are investigated in this section.

3.1. Nash equilibrium existence

To demonstrate existence of Nash equilibrium of a non-cooperative game, there are some Nash's existence theorems. In this paper, one of the commonly used methods to prove Nash equilibrium existence so-called Nikaido–Isoda theorem is adopted [41] as follows.

Theorem 1. *Consider the game with strategic form {A, $\mathbb{S}$, $\boldsymbol{u}_{DSO}$, $\boldsymbol{u}_{A_i}$, $\boldsymbol{u}_{D_i}$}. Assume conditions (a) and (b) are satisfied.*

(a) $\mathbb{S}_{DSO}$, $\mathbb{S}_{A_i}(\forall i = 1, 2, \cdots, a)$, and $\mathbb{S}_{D_i}(\forall i = 1, 2, \cdots, d)$ i.e. sets of strategy profiles of DSO, AC MGO_i, and DC MGO_i are nonempty, compact, and convex.

(b) $\mathscr{U}_{DSO}(\boldsymbol{u})$, $\mathscr{U}_{A_i}(\boldsymbol{u})$ $(\forall i = 1, 2, \cdots, a)$, and $\mathscr{U}_{D_i}(\boldsymbol{u})$ $(\forall i = 1, 2, \cdots, d)$ i.e. utility functions of DSO, AC MGO_i, and DC MGO_i are concave (The function f is concave if $(-f)$ is convex) and continuous.

Then there is at least one equilibrium.

In what follows, proof of conditions (a) and (b) of Theorem 1 for the defined problem in the paper are presented.

Proof (a): According to [40], the strategy spaces $\mathbb{S}_{DSO}$ and $\mathbb{S}_{A_i}$ ($\forall i = 1, 2, \cdots, a$) are bounded by the finite set of linear constraints and the second-order cone programming (SOCP) constraint. Also, the strategy space $\mathbb{S}_{D_i}(\forall i = 1, 2, \cdots, d)$ is bounded by the finite set of linear constraints and the SOCP constraint. Therefore, the strategy spaces $\mathbb{S}_{DSO}$, $\mathbb{S}_{A_i}(\forall i)$, and $\mathbb{S}_{D_i}(\forall i)$ are nonempty and compact. Furthermore, a linear constraint is clearly convex and SOCP is one of the well-known convex forms [42]. Thus, the strategy spaces of DSO and MGOs are convex.

Proof (b): According to (2) $\mathscr{U}_{DSO} = -f_{DSO}$, $\mathscr{U}_{A_i} = -f_{A_i}$, and $\mathscr{U}_{D_i} = -f_{D_i}$. Hence, the concavity of $\mathscr{U}_{DSO}$, $\mathscr{U}_{A_i}$, and $\mathscr{U}_{D_i}$ is resulted from the convexity of f_{DSO}, f_{A_i}, f_{D_i}. According to (3), each of f_{DSO}, f_{A_i}, and f_{D_i} is the summation of convex functions (P^{ls}_1 that is linear and therefore convex). Since the summation of convex functions is convex [42], f_{DSO}, f_{A_i}, and f_{D_i} are convex. On the other hand, a convex function is continuous [42]. Therefore, the convexity of f_{DSO}, f_{A_i}, and f_{D_i} result in the continuity of them and therefore, the continuity of $\mathscr{U}_{DSO}$, $\mathscr{U}_{A_i}$, and $\mathscr{U}_{D_i}$.

3.2. Convergence of proposed decentralized algorithm

Suppose that $i, j \in \{1, 2, \cdots, a\}$ are indices for AC MGOs and $k, l \in \{1, 2, \cdots, d\}$ are DC MGOs indices. To prove the convergence of the decentralized algorithm to the NE of the non-cooperative game, it should be noted that each player determines its optimal strategy in each iteration, assuming that the optimal strategies of all other players have been previously determined and fixed. Thus, in the n^{th} iteration, the best strategy of AC MGO_i and DC MGO_k regarding the other players' strategies chosen in $(n-1)^{th}$ iteration are as follows:

$$\boldsymbol{u}_{A_i}{}^{(n)} = \operatorname{argmax}_{\boldsymbol{u}_{A_i}} \mathscr{U}_{A_i}(\boldsymbol{u}_{DSO}{}^{(n-1)}, \boldsymbol{u}_{A_i}, \boldsymbol{u}_{A_{j\neq i}}{}^{(n-1)}, \boldsymbol{u}_{D_k}{}^{(n-1)}) \quad \forall i = 1, 2, \cdots, a \tag{31}$$

$$\boldsymbol{u}_{D_k}{}^{(n)} = \operatorname{argmax}_{\boldsymbol{u}_{D_k}} \mathscr{U}_{D_k}(\boldsymbol{u}_{DSO}{}^{(n-1)}, \boldsymbol{u}_{A_i}{}^{(n-1)}, \boldsymbol{u}_{D_k}, \boldsymbol{u}_{D_{l\neq k}}{}^{(n-1)}) \quad \forall k = 1, 2, \cdots, d \tag{32}$$

Likewise, the best strategy of DSO, $\boldsymbol{u}_{DSO}{}^{(n)}$ for the MGOs selected strategies $\boldsymbol{u}_{A_i}{}^{(n)}$ $(\forall i)$ and $\boldsymbol{u}_{D_k}{}^{(n)}$ $(\forall k)$ is as Eq. (33).

$$\boldsymbol{u}_{DSO}{}^{(n)} = \operatorname{argmax}_{\boldsymbol{u}_{DSO}} \mathscr{U}_{DSO}(\boldsymbol{u}_{DSO}, \boldsymbol{u}_{A_i}{}^{(n)}, \boldsymbol{u}_{D_k}{}^{(n)}) \tag{33}$$

Each player, DSO, AC MGO_i, or DC MGO_k will update its own strategy to a new strategy $\boldsymbol{u}_{DSO}{}^{(n+1)}$, $\boldsymbol{u}_{A_i}{}^{(n+1)}$, or $\boldsymbol{u}_{D_k}{}^{(n+1)}$ if and only if the new strategy increases its own utility function i.e.

$$\mathscr{U}_{A_i}\left(\boldsymbol{u}_{DSO}{}^{(n)}, \boldsymbol{u}_{A_i}{}^{(n+1)}, \boldsymbol{u}_{A_{j\neq i}}{}^{(n)}, \boldsymbol{u}_{D_k}{}^{(n)}\right) \geq \mathscr{U}_{A_i}\left(\boldsymbol{u}_{DSO}{}^{(n)}, \boldsymbol{u}_{A_i}{}^{(n)}, \boldsymbol{u}_{A_{j\neq i}}{}^{(n)}, \boldsymbol{u}_{D_k}{}^{(n)}\right) \quad \forall i = 1, 2, \cdots, a \tag{34-a}$$

$$\mathscr{U}_{D_k}\left(\boldsymbol{u}_{DSO}{}^{(n)}, \boldsymbol{u}_{A_i}{}^{(n)}, \boldsymbol{u}_{D_k}{}^{(n+1)}, \boldsymbol{u}_{D_{l\neq k}}{}^{(n)}\right) \geq \mathscr{U}_{D_k}\left(\boldsymbol{u}_{DSO}{}^{(n)}, \boldsymbol{u}_{A_i}{}^{(n)}, \boldsymbol{u}_{D_k}{}^{(n)}, \boldsymbol{u}_{D_{l\neq k}}{}^{(n)}\right)$$
$$\forall k = 1, 2, \cdots, d \tag{34-b}$$

$$\mathscr{U}_{DSO}\left(\boldsymbol{u}_{DSO}{}^{(n+1)}, \boldsymbol{u}_{A_i}{}^{(n+1)}, \boldsymbol{u}_{D_k}{}^{(n+1)}\right) \geq \mathscr{U}_{DSO}\left(\boldsymbol{u}_{DSO}{}^{(n)}, \boldsymbol{u}_{A_i}{}^{(n+1)}, \boldsymbol{u}_{D_k}{}^{(n+1)}\right) \tag{34-c}$$

With the definition of the gap between the utility function at n^{th} iteration and the maximum utility function as

$$\Delta\mathscr{U}_{A_i}{}^{(n)} = \mathscr{U}_{A_i}\left(\boldsymbol{u}_{DSO}{}^{(n-1)}, \boldsymbol{u}_{A_i}{}^{(n)}, \boldsymbol{u}_{A_{j\neq i}}{}^{(n-1)}, \boldsymbol{u}_{D_k}{}^{(n-1)}\right) - \mathscr{U}_{A_i}(\boldsymbol{u}^\star)$$
$$\forall i = 1, 2, \cdots, a \tag{35-a}$$

$$\Delta\mathscr{U}_{D_k}{}^{(n)} = \mathscr{U}_{D_k}\left(\boldsymbol{u}_{DSO}{}^{(n-1)}, \boldsymbol{u}_{A_i}{}^{(n-1)}, \boldsymbol{u}_{D_k}{}^{(n)}, \boldsymbol{u}_{D_{l\neq k}}{}^{(n-1)}\right) - \mathscr{U}_{D_k}(\boldsymbol{u}^\star)$$
$$\forall k = 1, 2, \cdots, d \tag{35-b}$$

$$\Delta\mathscr{U}_{DSO}{}^{(n)} = \mathscr{U}_{DSO}\left(\boldsymbol{u}_{DSO}{}^{(n)}, \boldsymbol{u}_{A_i}{}^{(n)}, \boldsymbol{u}_{D_k}{}^{(n)}\right) - \mathscr{U}_{DSO}(\boldsymbol{u}^\star) \tag{35-c}$$

The gap is written as Eq. (36) for $(n+1)^{th}$ iteration.

$$\Delta\mathscr{U}_{A_i}{}^{(n+1)} = \mathscr{U}_{A_i}\left(\boldsymbol{u}_{DSO}{}^{(n)}, \boldsymbol{u}_{A_i}{}^{(n+1)}, \boldsymbol{u}_{A_{j\neq i}}{}^{(n)}, \boldsymbol{u}_{D_k}{}^{(n)}\right) - \mathscr{U}_{A_i}(\boldsymbol{u}^\star)$$
$$\forall i = 1, 2, \cdots, a \tag{36-a}$$

$$\Delta\mathscr{U}_{D_k}{}^{(n+1)} = \mathscr{U}_{D_k}\left(\boldsymbol{u}_{DSO}{}^{(n)}, \boldsymbol{u}_{A_i}{}^{(n)}, \boldsymbol{u}_{D_k}{}^{(n+1)}, \boldsymbol{u}_{D_{l\neq k}}{}^{(n)}\right) - \mathscr{U}_{D_k}(\boldsymbol{u}^\star)$$
$$\forall k = 1, 2, \cdots, d \tag{36-b}$$

$$\Delta\mathscr{U}_{DSO}{}^{(n+1)} = \mathscr{U}_{DSO}\left(\boldsymbol{u}_{DSO}{}^{(n+1)}, \boldsymbol{u}_{A_i}{}^{(n+1)}, \boldsymbol{u}_{D_k}{}^{(n+1)}\right) - \mathscr{U}_{DSO}(\boldsymbol{u}^\star) \tag{36-c}$$

By subtracting $\mathscr{U}_{A_i}(\boldsymbol{u}^\star)$ from both sides of (34-a), we have.

$$\mathscr{U}_{A_i}\left(\boldsymbol{u}_{DSO}{}^{(n)}, \boldsymbol{u}_{A_i}{}^{(n+1)}, \boldsymbol{u}_{A_{j\neq i}}{}^{(n)}, \boldsymbol{u}_{D_k}{}^{(n)}\right) - \mathscr{U}_{A_i}(\boldsymbol{u}^\star)$$
$$\geq \mathscr{U}_{A_i}\left(\boldsymbol{u}_{DSO}{}^{(n)}, \boldsymbol{u}_{A_i}{}^{(n)}, \boldsymbol{u}_{A_{j\neq i}}{}^{(n)}, \boldsymbol{u}_{D_k}{}^{(n)}\right) - \mathscr{U}_{A_i}(\boldsymbol{u}^\star) \Rightarrow \Delta\mathscr{U}_{A_i}{}^{(n+1)} \geq \Delta\mathscr{U}_{A_i}{}^{(n)} \tag{37-a}$$

and by subtracting $\mathscr{U}_{D_k}(\boldsymbol{u}^\star)$ from both sides of (34-b), we can obtain.

$$\mathscr{U}_{D_k}\left(\boldsymbol{u}_{DSO}{}^{(n)}, \boldsymbol{u}_{A_i}{}^{(n)}, \boldsymbol{u}_{D_k}{}^{(n+1)}, \boldsymbol{u}_{D_{l\neq k}}{}^{(n)}\right) - \mathscr{U}_{D_k}(\boldsymbol{u}^\star)$$
$$\geq \mathscr{U}_{D_k}\left(\boldsymbol{u}_{DSO}{}^{(n)}, \boldsymbol{u}_{A_i}{}^{(n)}, \boldsymbol{u}_{D_k}{}^{(n)}, \boldsymbol{u}_{D_{l\neq k}}{}^{(n)}\right) - \mathscr{U}_{D_k}(\boldsymbol{u}^\star) \Rightarrow \Delta\mathscr{U}_{D_i}{}^{(n+1)} \geq \Delta\mathscr{U}_{D_i}{}^{(n)} \tag{37-b}$$

Likewise, by subtracting $\mathscr{U}_{DSO}(\boldsymbol{u}^\star)$ from both sides of (34-c), it can be written.

$$\mathscr{U}_{DSO}\left(\boldsymbol{u}_{DSO}{}^{(n+1)}, \boldsymbol{u}_{A_i}{}^{(n+1)}, \boldsymbol{u}_{D_k}{}^{(n+1)}\right) - \mathscr{U}_{DSO}(\boldsymbol{u}^\star)$$
$$\geq \mathscr{U}_{DSO}\left(\boldsymbol{u}_{DSO}{}^{(n)}, \boldsymbol{u}_{A_i}{}^{(n+1)}, \boldsymbol{u}_{D_k}{}^{(n+1)}\right) - \mathscr{U}_{DSO}(\boldsymbol{u}^\star) \Rightarrow \Delta\mathscr{U}_{DSO}{}^{(n+1)} \geq \Delta\mathscr{U}_{DSO}{}^{(n)} \tag{37-c}$$

Or briefly.

$$\Delta\mathscr{U}_{A_i}{}^{(n)} \leq \Delta\mathscr{U}_{A_i}{}^{(n+1)} \leq 0 \quad \forall i = 1, 2, \cdots, a \tag{38-a}$$

$$\Delta\mathscr{U}_{D_k}{}^{(n)} \leq \Delta\mathscr{U}_{D_k}{}^{(n+1)} \leq 0 \quad \forall k = 1, 2, \cdots, d \tag{38-b}$$

$$\Delta\mathscr{U}_{DSO}{}^{(n)} \leq \Delta\mathscr{U}_{DSO}{}^{(n+1)} \leq 0 \tag{38-c}$$

The players iteratively update their own strategies and the best strategy result in a non-decreasing sequence of changes in the utility function as

$$\{\Delta\mathscr{U}_{A_i}{}^{(1)}, \Delta\mathscr{U}_{A_i}{}^{(2)}, \cdots, \Delta\mathscr{U}_{A_i}{}^{(n)}, \cdots\} \ \forall i = 1, 2, \cdots, a \tag{39-a}$$

$$\{\Delta\mathscr{U}_{D_k}{}^{(1)}, \Delta\mathscr{U}_{D_k}{}^{(2)}, \cdots, \Delta\mathscr{U}_{D_k}{}^{(n)}, \cdots\} \quad \forall k = 1, 2, \cdots, d \tag{39-b}$$

$$\{\Delta\mathscr{U}_{DSO}{}^{(1)}, \Delta\mathscr{U}_{DSO}{}^{(2)}, \cdots, \Delta\mathscr{U}_{DSO}{}^{(n)}, \cdots\} \tag{39-c}$$

As the utility function of any player is bounded, the above sequences eventually converge to a solution that further improvement in the utility functions is impossible. This point is the Nash equilibrium solution of the game. In other words, we have $\limsup_{n\to\infty} \Delta\mathscr{U}_{DSO}{}^{(n)} = 0$, $\limsup_{n\to\infty} \Delta\mathscr{U}_{A_i}{}^{(n)} = 0$, and $\limsup_{n\to\infty} \Delta\mathscr{U}_{D_k}{}^{(n)} = 0$. Therefore, the proof is completed.

4. Simulations and results

The main focus of our paper is to develop a coordinated decentralized framework for loss minimization in distribution networks including both AC and DC microgrids. The modified IEEE 69-bus test network considering one DC microgrid and three AC microgrids is employed to evaluate the competency of the model as shown in Fig. 5. The required network data is extracted from [43]. The required data of the aforementioned distribution system are given in Table I. The allowable voltage range is assumed to be between 0.9 and 1.1p.u. The distribution system and microgrids consist of various dispatchable and non-dispatchable DERs and VAR compensators as well which can participate in loss minimization of distribution systems and microgrids through their active/reactive power capabilities. This paper considers DERs with various reactive power capability curves. For instance, for SDGs we have $\mathfrak{a} = \mathfrak{b} = 0.62$, $\alpha = \beta = 3.51$, $\widetilde{Q}^{dg}$=0 and for PV DGs the reactive power capability curves are described by $\mathfrak{a} = 0.33$, $\mathfrak{b} = 0.48$, $\alpha = 2.81$, $\beta = 2.31$, $\widetilde{Q}^{dg}$=0.215 MVAr. The scheduled active and reactive power of SDGs are optimally calculated. Regarding renewables, there are many stochastic and robust methods for modeling the fluctuations in the output of renewable energy resources like PVs. This paper assumes that active power outputs of renewables have been previously determined using a stochastic or robust method and they are assumed to be known and fixed and just reactive power share of renewable, based on their reactive power capability curves, are determined. All of the defined sub-problems for AC MGs, DC MGs, and DSO have been solved in GAMS software through KNITRO solver to schedule the next hour period. The boundary variable's amounts, active exchanged power and voltage magnitude in different iterations of the proposed algorithm, are depicted in Fig. 6. As this figure shows, all boundary variables reach to their final values after four iterations. The scheduled active power transaction between distribution network and AC MG1, AC MG2, AC MG3, and DC microgrids are −0.065, −0.046, 0.144, and 0.5416 MW respectively. It means that AC MG1 and AC MG2 receive active power from distribution network while AC MG3 and DC MG send active power to the distribution system. This power exchange, as mentioned before, is conducted so that DSO and also each MGO can minimize its own objective function i.e. active power loss. Fig. 7 represents the objective function values of different players at the equilibrium point where all the players are satisfied with their solutions. The voltage of buses belong to the distribution network, AC MG1 and DC MG have been reported in Fig. 8. As it can be observed, the obtained voltage values are completely within the allowable range.

Fig. 9 illustrates both total active and reactive generated power of different stakeholders. As observed, AC MG3 and DC MG are the main suppliers of active power for the whole distribution network. Moreover, AC MG3 along with distribution network have the role of reactive power compensation in an integrated system since these networks are equipped with DG and VAr compensator.

4.1. Effect of considering ZIP load models

In previous case studies, losses are minimized by increasing the voltage at the substation because demand is modeled as constant power loads. In this sub-section, another case is studied in which MGOs require modeling their loads as voltage dependent, but the DSO doesn't. For this purpose, the following two cases are compared.

- Case 1: All loads in the distribution network and microgrids are constant power.
- Case 2: Loads of microgrids are voltage-dependent (using ZIP model) while loads of distribution networks are still constant power.

Results of active power losses and voltage profiles of grids in these two cases are compared in Fig. 10 and Fig. 11, respectively. According to

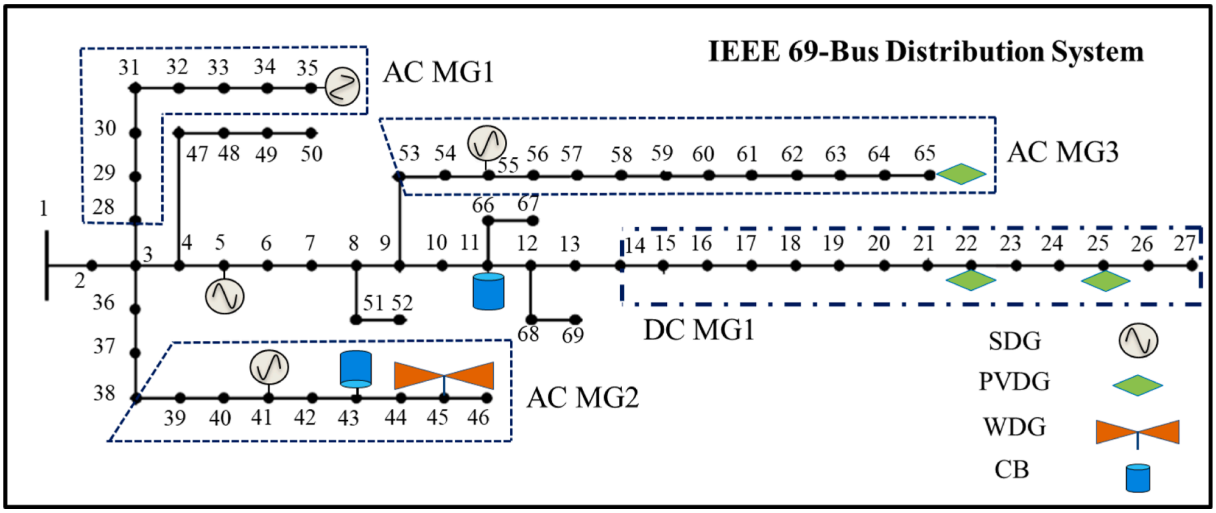

Fig. 5. The modified IEEE 69-bus network with multiple AC and DC microgrids.

Table 1
The required data of the distribution system.

Network	*Load*		*Active/Reactive Resource Capacity*			
	Active (MW)	*Reactive (MVar)*	*SDG (MVA)*	*WDG (MW)*	*PVDG (MW)*	*CB (MVar)*
Dist. Net	1.511	1.08	0.3	–	–	[0, 0.6]
AC MG1	0.092	0.065	0.1	–	–	–
AC MG2	0.134	0.092	0.6	0.4	–	[0, 0.6]
AC MG3	1.717	1.227	4	–	0.5	–
DC MG	0.35	–	–	–	0.4 @ bus 22 0.5 @ bus 25	–

Fig. 10, in Case 2 that MGOs' loads are voltage-dependent, satisfying loads increase voltage level of microgrids and distribution system which in turn leads to the decrease of active power losses of each player's network. For example, reduction in active power losses for networks managed by DSO, AC MG3, and DC MG is 39%, 6.5%, and 10.7% respectively in comparison with case 1. Also, the active power reduction of the whole network is about 19 % compared to case 1 where all loads are active power constants.

4.2. Effect of DG penetration

To investigate the sensitivity of the final solution to the characteristics of the players, especially total DG penetration of each network, the coordinated problem has been also solved for various DG penetrations. For this purpose, 10 cases have been simulated. In base case 7 (same as the case studied in the previous sections), the capacity of synchronous DGs are according to Table 1 and for other cases, the base DG capacities are multiplied by a DG factor according to Table 2. Other parameters are maintained constant in all cases.

Fig. 12 shows that as DERs penetration increases, total power losses of the network first decreases and then increases and finally saturates. The variation of power losses by changing the penetration of DERs for the distribution network is same as the whole network. However, AC MG3 and DC MG have the opposite behaviour in comparison with distribution network, where power loss first increases and then decreases, although the worst case of power loss does not occur at the same DG penetration. The worst power losses for AC MG3 is associated with DG factor = 0.4 while it occurs at DG factor = 1.1 for DC MG. As the penetration of DGs increases, power losses of AC MG1 and AC MG2 have decreasing and increasing behaviour, respectively. Therefore, different players have different sensitivity to the penetration of DGs and it depends on the characteristics of the players and network such as the configuration of networks, load demand, etc. Furthermore, players are self-interested and each player tries to individually minimize the power loss of its own network and therefore, the decrease of power loss for one player may lead to the increase of power loss of others.

4.3. Discussion on the computational performance of the proposed method and robustness against initial conditions

This sub-section aims to evaluate the efficiency of the proposed method from computational performance aspect. To this end, the algorithm is run taking into account different initial condition. The robustness of the proposed algorithm in terms of initial condition has been indicated in Fig. 13. The proposed decentralized algorithm is an ultra-high speed algorithm in comparison with other decentralized methods due to the fact that the convergence obtained in 2–4 iterations. It is notable that the previous introduced decentralized algorithms in [33,35,36] and [39] are converged in at least 170, 30, 80, and 40 iterations, respectively. This great achievement is because of eliminating the direct insertion of consistency constraints though splitting and devoting boundary variables to the related stakeholders considering a transactive procedure as discussed before.

It should be noted that In the decentralized optimization methods, such as ADMM method, consistency constraints are added to ensure the matching of boundary variables in the relevant sub-problems. Satisfaction of these constraints is a necessity for the convergence of the decentralized method (in addition to convergence of objective functions of different agents). Usually, all boundary variables are decided by all involved agents. An agent calculates a value for a given boundary variable (e.g. voltage of boundary bus) and the other agent (s) on other side of the boundary tries to follow the boundary variables obtained by the first agent. This approach of matching boundary variables increases the number of iterations and therefore the solution time. Also, the

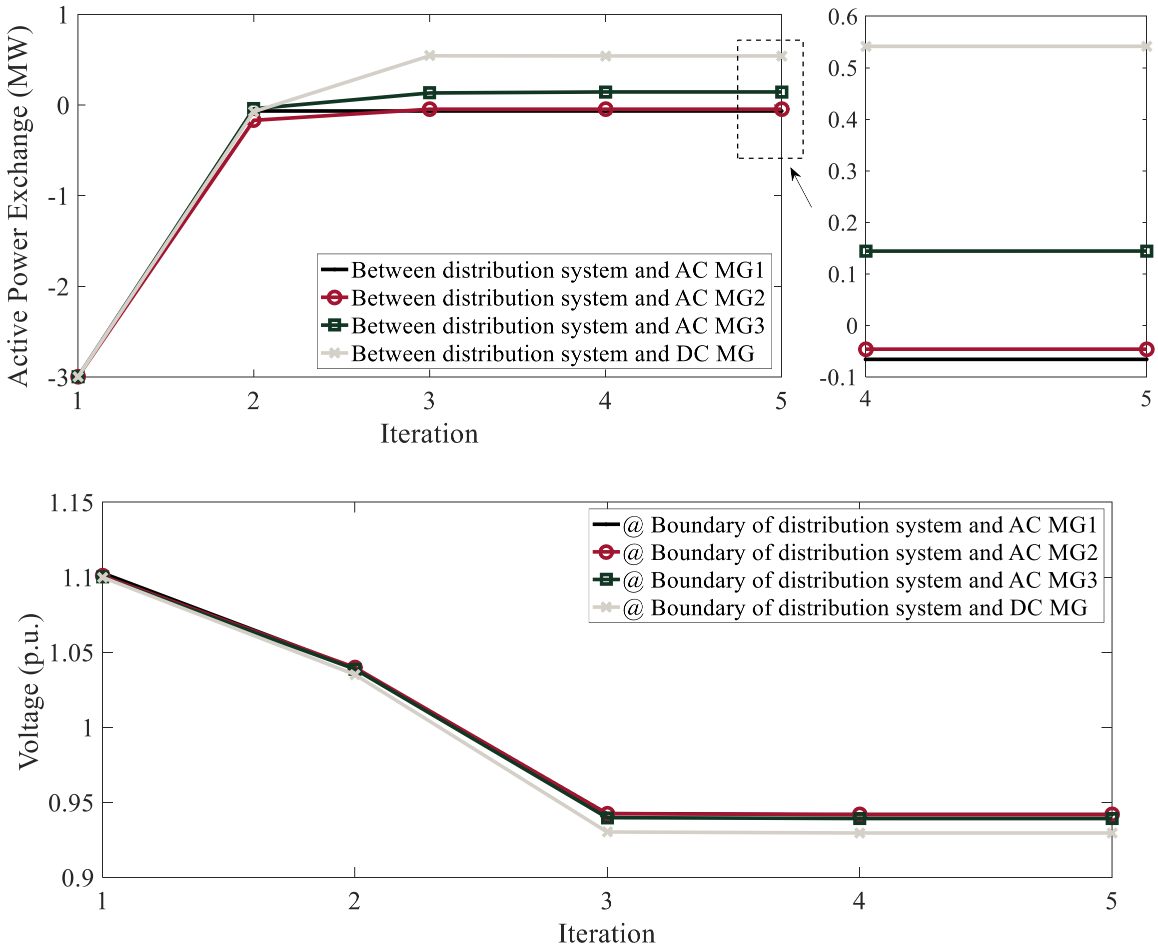

Fig. 6. The obtained values for the boundary variables.

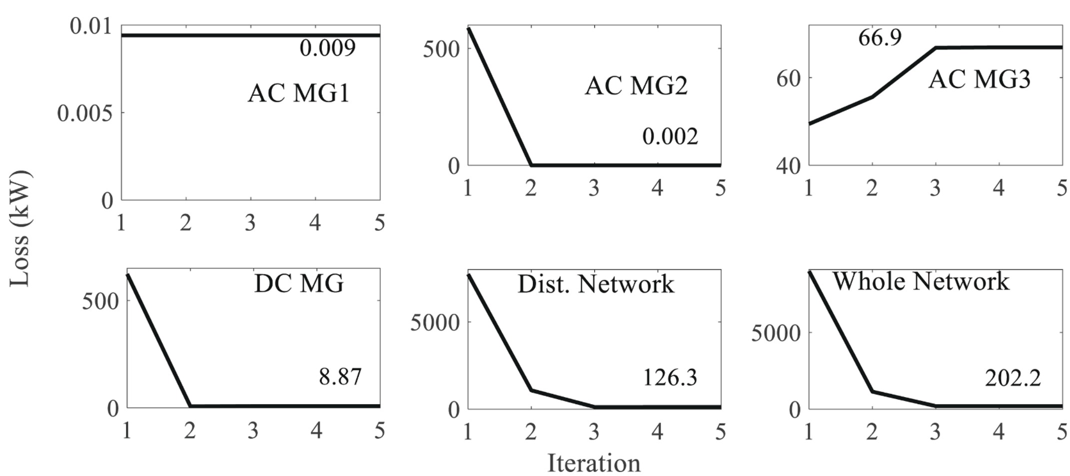

Fig. 7. The active power loss of distribution network and MGs.

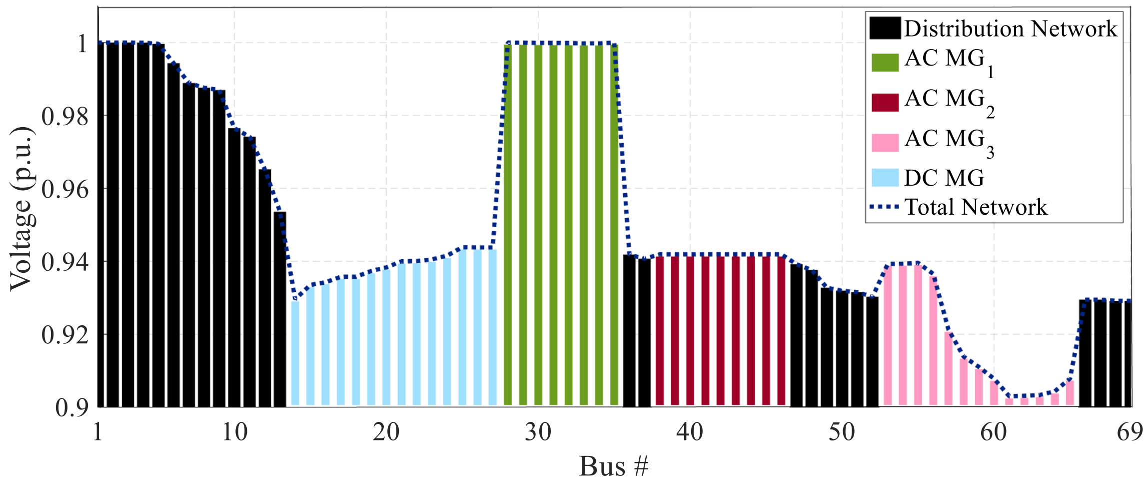

Fig. 8. Voltage magnitude of buses associated with MGs and distribution network.

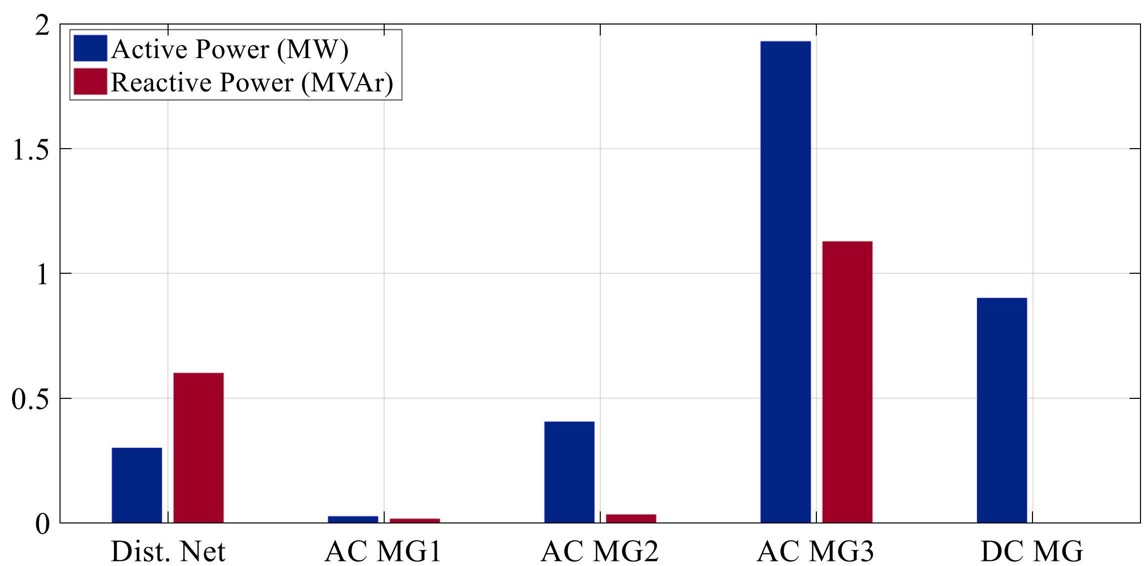

Fig. 9. Active/reactive power scheduling of different stakeholders.

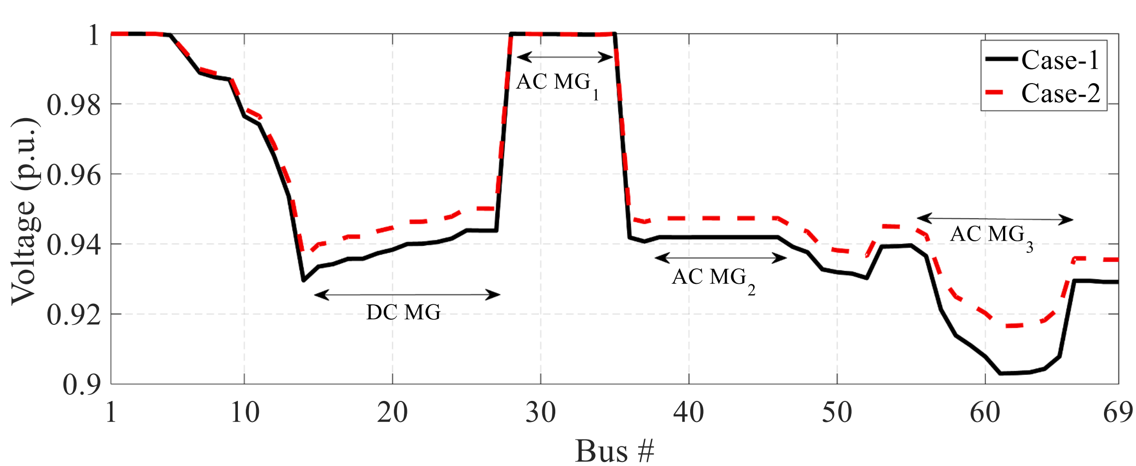

Fig. 10. Comparison of voltage magnitude of the network in Cases 1 and Case2.

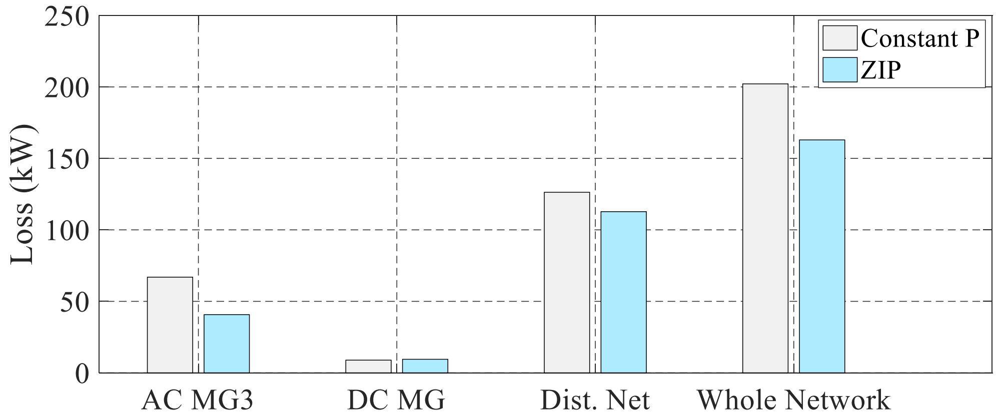

Fig. 11. Active power loss Comparison among distribution network and some MGs in Cases 1 and 2.

Table 2
DG Factor in Cases 1–10.

Case	1	2	3	4	5	6	**7**	8	9	10
DG factor	0.1	0.2	0.4	0.6	0.7	0.9	**1**	1.1	1.2	1.3

conventional decentralized methods have some parameters that directly affect the convergence of the problem. Therefore, to decrease the iteration numbers and at the sane tine keep the accuracy, such parameters need to be tuned suitably. This paper introduces PABI technique to match boundary variables. This method neither has any parameters to be tuned nor need to insert the consistency constraints directly in subproblems of involved agents, because boundary variables of each boundary are categorized into two groups. Each group of boundary variables is decided by one decision-maker and shared by others to use it. This property can speed up the convergence of the interactive decentralized method. In addition, in contrast to decentralized methods like ADMM, there is not a need for the setting of some parameters. Moreover, reducing the number of variables to be shared between DSO and each MGO is another merit of the proposed method. A consequence of this is reducing the communication burden of the interactions between DSO and MGOs.

The initial values in Fig. 6 and initial values of some cases in Fig. 13 are intentionally exaggerated. To clarify this, the following discussion is provided. In fact, regardless of the beginner of the algorithm (DSO or MGOs) or the initial values which supposed by the beginner, the algorithm is converged to the same solution i.e. 0.2 MW active power losses of the total system. In other words, it is one of the main properties of the proposed decentralized algorithm that is robust against the initial conditions. For example, for the cases that the algorithm is initiated by DSO, it needs to assume some initial values for active and (or) reactive power exchange with AC and DC microgrids. Fig. 13 shows that even if DSO assumes large values for these boundary variables which leads to the infeasible solution (e.g 8–9 MW at the first iteration of Fig. 6 and some cases of Fig. 13), the algorithm is able to gradually modify the boundary variables to the feasible ones and finally converges to the optimal values. This is the value of the interaction that DSO and MGOs can share boundary variables (even if the initial boundary variables are infeasible) to and receive feedback from each other to modify their solutions and finally converge to the equilibrium point. At this point, the values of individual and boundary variables of each player are feasible and satisfy all constraints and furthermore, none of the players can improve its objective function with respect to the previous iteration and the equilibrium is achieved.

As another important point, it is well known and provable that the

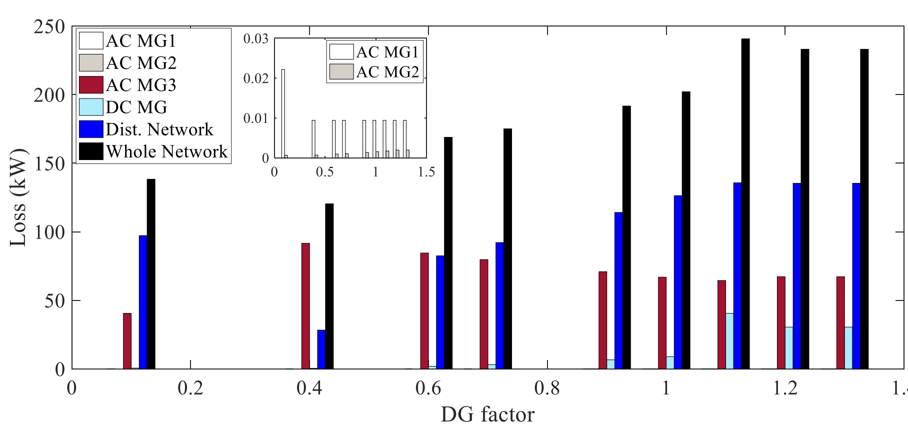

Fig. 12. Sensitivity of the final solution of different players to DER penetration.

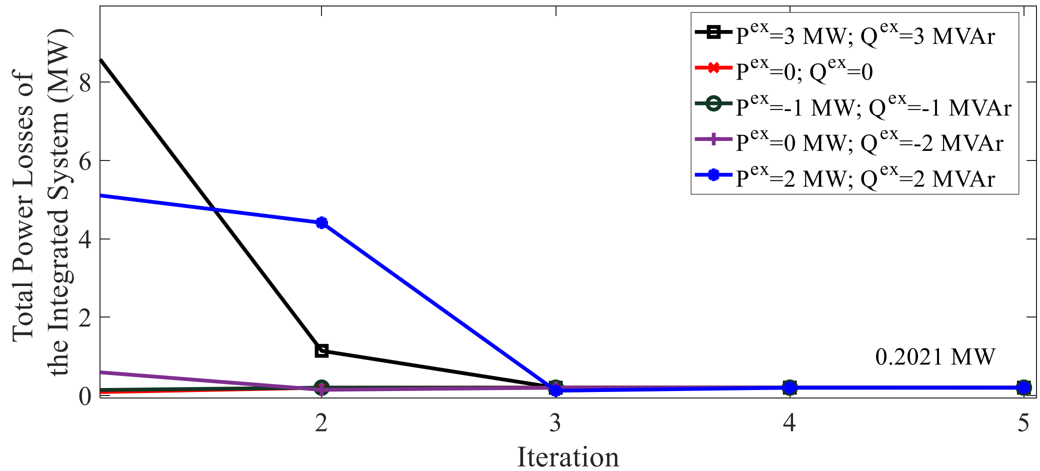

Fig. 13. Comparison the convergence of the proposed scheme for distribution network with multiple MGs for some initial conditions.

real power losses in the electric network decrease with the increase of the voltage level of the grid, but the results presented in Fig. 5 and Fig. 6 show that real power losses decrease from one iteration to the other with a dramatic decrease in the voltage profile of the grid. However, Fig. 6 is related to one of the cases that *initial* active power exchange between distribution network and each microgrid is assumed 3 MW which is completely unrealistic and leads to the infeasible solution at *first* iterations. As mentioned before, cases like this are intentionally studied to illustrate the robustness of the proposed decentralized method against the initial conditions. However, the real power losses in the electric network decrease with the increase of the voltage level of the grid, and this can be exactly observed for cases that the initial conditions are feasible. For example, Fig. 14 shows the active power losses of the distribution system, AC-MG3 (for instance) and whole network for a feasible case in which constraints of all networks are satisfied. In this case, real power losses increase from one iteration to the other with a dramatic decrease in the voltage profile of the grid. Note that, the power losses of Fig. 14 converge to exactly the same values as in Fig. 6 and the difference of trend of curves are because of difference in initial conditions.

4.4. Applicability of the proposed method for multi-period scheduling problems

In general, VVO problem can be solved to minimize active power losses for one time slot or minimize active energy losses for multiple time slots or multi-period. The focus of the proposed method is solving the first one. However, it is able to handle multi-period scheduling problems.

In this subsection, to further show the advantage of the proposed method in solving VVO problem for distribution systems with multiple AC and DC microgrids, the case of multi-period scheduling is also studied. The problem is solved for one hour horizon with 4 time slots (each time slot equals 15 min). For this purpose, the following modifications have been made:

1) Objective functions are modified as

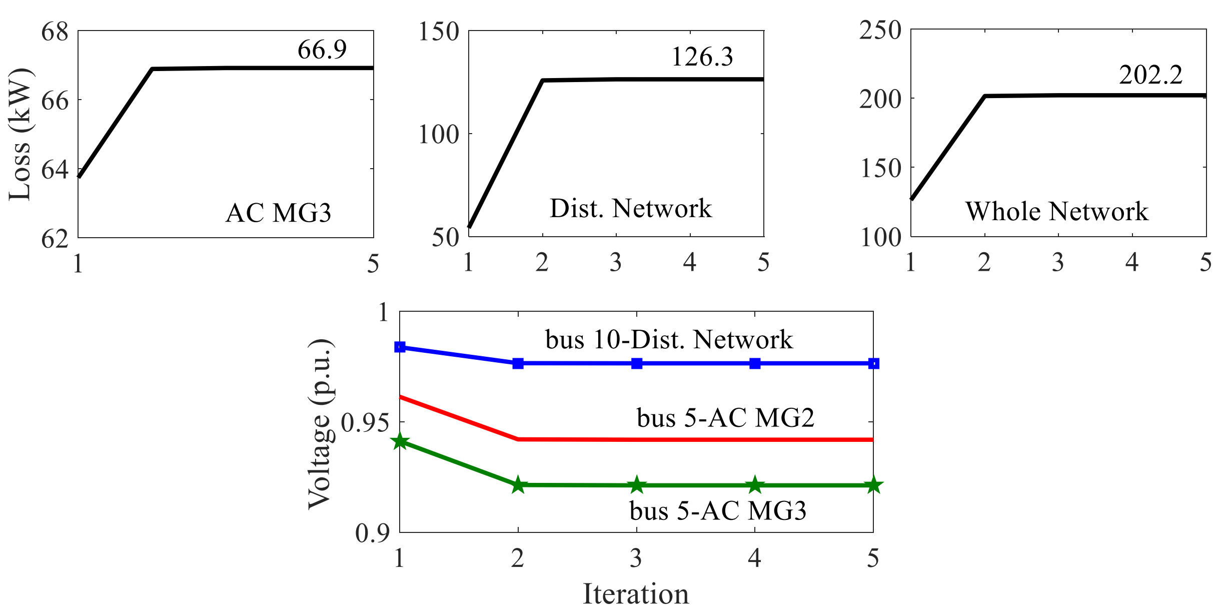

Fig. 14. Increase of real power losses from one iteration to the other with a dramatic decrease in the voltage profile of the grid.

$$\text{DSO}: \ \text{Min} f_{DSO} = \sum_{t \in \mathbb{T}} \sum_{l \in \mathbb{L}_{DSO}} P_l^{ls}(t) \Delta t \tag{40a}$$

$$\text{AC MGO } i: \ \text{Min} f_{A_i} = \sum_{t \in \mathbb{T}} \sum_{l \in \mathbb{L}_{A_i}} P_l^{ls}(t) \Delta t \tag{40b}$$

$$\text{DC MGO } i: \ \text{Min} f_{D_i} = \sum_{t \in \mathbb{T}} \Delta t (\sum_{l \in \mathbb{L}_{D_i}} P_l^{ls}(t) + P_c^{ls}(t)) \tag{40c}$$

where similar to [44], a second-order function as $P_c^{ls}(t) = \alpha_c I_c{}^2(t) + \beta_c I_c(t) + \gamma_c$ with the same parameter is considered for AC/DC converter.

2) Constraints of single-period problem are used for different time slots (t = 1, 2, 3, and 4).

3) Inter-temporal constraints are added to relate constraints of different time slots. For instance, constraints of energy storage systems (ESSs) are considered as follows

$$P_{i,t}^{ST} = P_{i,t}^{ch} - P_{i,t}^{dis} \tag{41a}$$

$$0 \le P_{i,t}^{ch} \le b_{i,t} P_i^{ch,max}, \ 0 \le P_{i,t}^{dis} \le (1 - b_{i,t}) P_i^{dis,max} \tag{41b}$$

$$E_{i,t} = E_{i,t-1} + P_{i,t}^{ch} \times \eta_{ch} - P_{i,t}^{dis} / \eta_{dis} \tag{41c}$$

$$E_i^{min} \le E_{i,t} \le E_i^{max} \tag{41d}$$

where $P_{i,t}^{ST}$, $P_{i,t}^{ch}$, and $P_{i,t}^{dis}$ are net, charging, and discharging power of ESS of bus i at time t. To consider ESS, $P_{i,t}^{ST}$ should be added to equality constant associated with active power balance. In (41b), $P_i^{ch,max}$/ $P_i^{dis,max}$ shows the maximum charging/ discharging rate of ESS. Binary variable $b_{i,t}$ demonstrates status of battery where $b_{i,t} = 1$ shows charging status while $b_{i,t} = 0$ indicates discharging of ESS. Equation (41c) defines energy (state of charge) of the ESS where η_{ch}/ η_{dis} shows charge/discharge efficiency. Finally, E_i^{min} and E_i^{max} are lower and upper limits of ESS's energy. Here, two ESSs with the same parameter ($P_i^{ch,max} = P_i^{dis,max} = 1\,\text{MW}$, $E_i^{min} = 0.15\,\text{MWh}$, $E_i^{max} = 1.5\,\text{MWh}$, $E_{i,0} = 0.5\,\text{MWh}$, and$\eta_{ch} = \eta_{dis} = 0.95$) are considered for AC MG3 @ bus 64 and DC MG @ bus 23.

4) To obtain different values for different time slots of the multi-period problem, load, WDG, and PVDG values in single-period problem are multiplied by the coefficients depicted in Fig. 15.

Results of the simulations for the case of multi-period problem are summarized in Figs. 16-18. The active power output of each ESS in each time slot in which the positive and negative signs respectively show charging and discharging of ESS are shown in Fig. 16 (a). Also, according to Fig. 16 (b), in all time slots, the energy of both ESSs is within the allowed range. Values of boundary variables especially active power exchange between the distribution system and each microgrid and voltage of boundary buses are depicted in Fig. 17. Finally, active power losses of distribution systems, microgrids, and the whole power network for different iterations of the proposed method are demonstrated in Fig. 18. Fig. 18 also shows the effect of ESSs on the active power losses of different sub-systems. If compared to Fig. 7, among microgrids, active power losses of AC MG 3 and DC MG are mainly affected by the presence of ESSs. In fact, ESS increases active power losses of AC MG3 while reducing active power losses of DC MG. Also, the discharge of ESS of AC MG3 that plays the role of a generation unit decreases active power losses of the distribution system, significantly. As Fig. 17 (a) shows, in all time slots (especially time slot 1), only AC MG3 exports active power to the distribution system which in turn helps active power reduction of the distribution system and therefore whole power network, although flowing the active power generated by ESS through lines of AC MG results in increasing active power losses of this microgrid.

As another important observation, as Fig. 18 shows, the proposed method could still preserve its high-speed convergence even in the case of a multi-period problem which confirms the applicability of the proposed method for solving the multi-period problem.

4.5. Comparison with other works

In the revised version of the paper, the proposed non-cooperative framework has been compared with the cooperative approach of DSOs and MGOs which is the focus of most of the works [10,33,34,36–39] in the field of DSO-MGOs coordination. In contrast to the proposed non-cooperative DSO-MGOs method in which all agents try to minimize active power losses of their own networks in a self-interested manner until an equilibrium is attained, the goal of cooperative methods is to minimize total active power losses of the whole network including distribution system, AC microgrids, and DC microgrids. In Table 3, these two approaches of coordination of distribution system and microgrids compared in terms of total active power losses, active power losses of distribution system, and active power losses of each AC and DC microgrids. According to the results present in Table 3, the following conclusions are derived:

- As expected, for the whole network including distribution system and all microgrids, the cooperative method attains lower active power losses in comparison to the non-cooperative method because summation of active power losses of the whole system is minimized.
- Regarding the distribution network, the active power losses in the cooperative method is about 3.86% lower than those of the non-cooperative method because summation of active power losses are minimized in cooperative method and active power losses of distribution system has a significant share of the objective function.
- The proposed non-cooperative methods obtains lower active power losses for each microgrid with respect to the cooperative method because in the non-cooperative method each agent (DSO or MGOs) selfishly tries to minimize its own objective function even it has a lower relative share of total objective function. The decrease in active power losses of AC MG1, AC MG2, AC MG3, and DC MG is about 91.8%, 98.57%, 3.33%, and 11.38% when they prefer non-

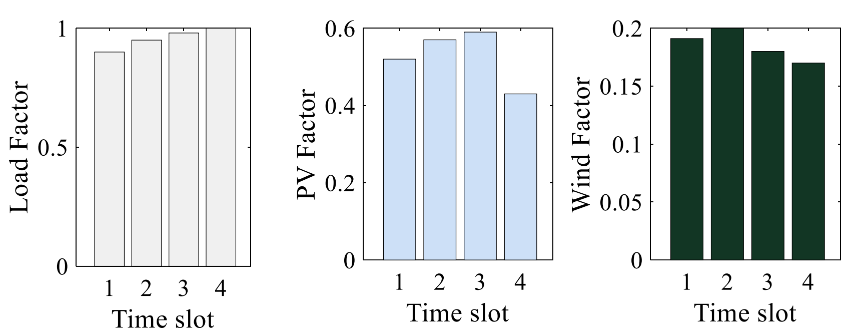

Fig. 15. Coefficients of load, PVDG, and WDG for multi-period case.

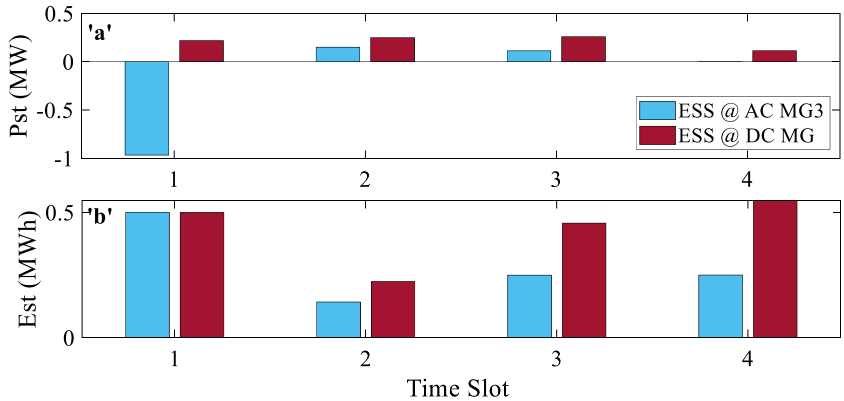

Fig. 16. Output of ESSs in terms of charging/ discharging power (positive sign shoes charging state) and energy (state of charge) for different time slots of multi-period case.

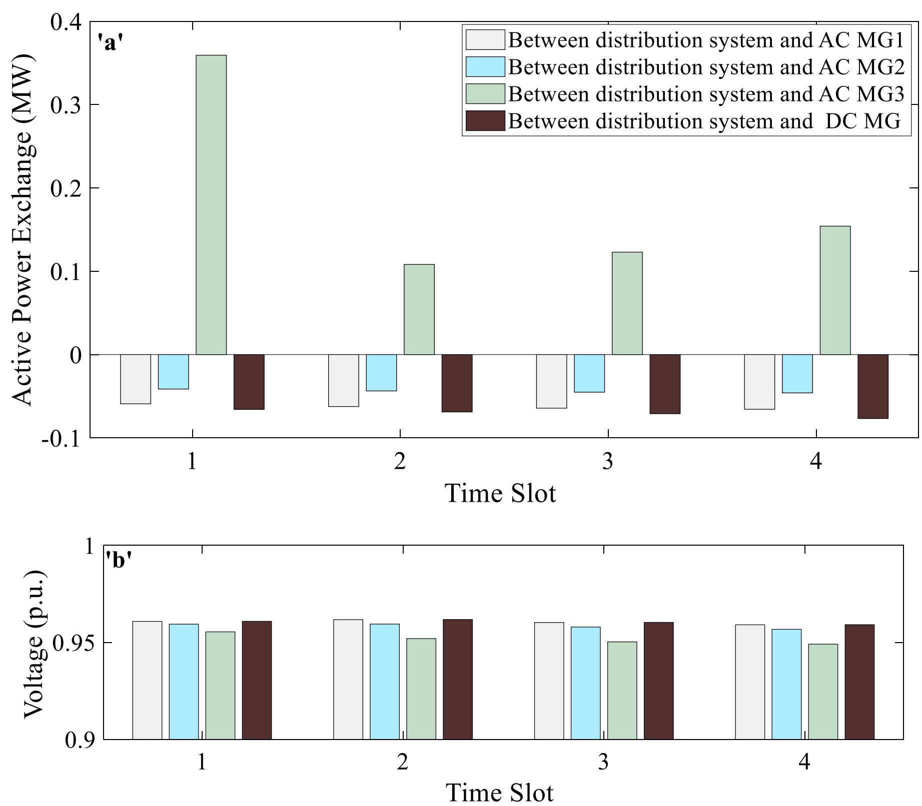

Fig. 17. Boundary variables a) active power exchange, and b) voltage at boundary of active distribution system and each microgrid for different time slots of multi-period case.

cooperation approach to cooperative method for the coordination with DSO.

- Although the minimum active power losses of whole system is obtained by cooperative method because of its system-wise nature, the solution of non-cooperative method is also suitable from a system-wise perspective (the difference is below 0.5%). On the other hand, in the cooperative method some agents (MGOs) are not satisfied while in non-cooperative method, due to its self-interested nature, all agents are satisfied with their solutions.

In overall, the selection of cooperative or non-cooperative method for the coordination of DSO and MGOs completely depends on the attitude of the agents to the coordination problem. In a system-wise approach, minimization of the whole system is more important and the cooperative method is preferred. However, in an agent wise-approach, agents prefer to take care of its own objective functions selfishly. It should be noted that, according to Table 3, the non-cooperative. In this regard, this paper introduces a new approach of coordination of DSO and MGOs besides the cooperative method which has been investigated in most of the existing works to give a better insight for system operators (DSOs and MGOs) when thinking about the coordination problem.

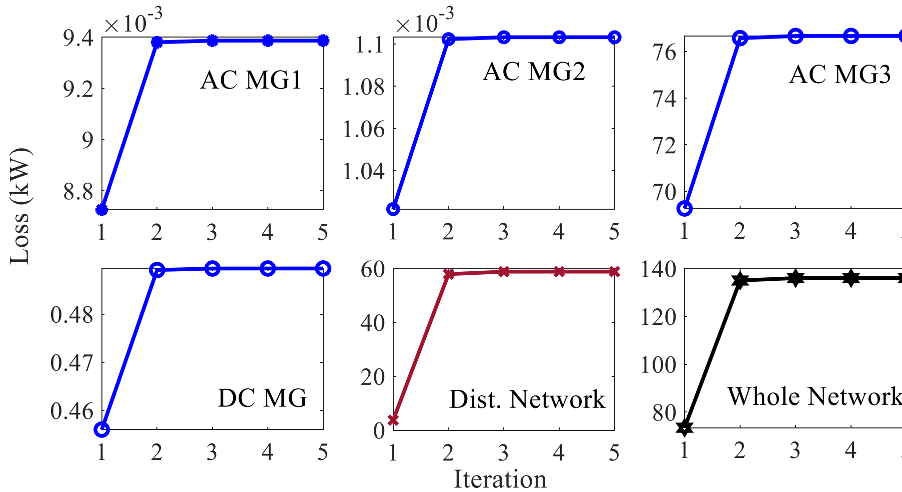

Fig. 18. The active power loss of distribution network and MGs for multi-period case.

Table 3
Comparison of the poroised non-cooperated method with cooperative methods.

Approach	***Active power losses (kW)***					
	Whole Net.	*Dist. Net*	*AC MG1*	*AC MG2*	*AC MG3*	*DC MG*
Cooperative	201.14	121.6	0.11	0.21	69.21	10.01
Non-Cooperative	202.1	126.3	0.009	0.002	66.9	8.87
VONC (%)	+ 0.47 %	+ 3.86%	−91.8%	−98.57 %	−3.33 %	−11.38%

* VONC (Value of non-cooperation) = 100*(Value in non-cooperative approach - Value in cooperative approach) / Value in cooperative approach.

5. Conclusion

A decentralized coordinated framework was presented for VVO of distribution systems with several AC and DC microgrids in the presence of DERs. The paper developed a non-cooperative scheme to coordinate MGOs and DSO so that all system operators all self-interested and try to minimize active power losses of their associated networks selfishly while they interactively share boundary variables to improve their solutions and satisfy both individual and boundary constraints. Furthermore, the proposed coordination scheme was implemented based on a new decentralized algorithm called PABI in which boundary variables are suitably portioned and assigned to relevant players. Numerical studies demonstrate that the proposed coordination framework can efficiently obtain a satisfactory solution in which active power losses for distribution network and AC and DC microgrids are minimized and constraints of all networks are satisfied. Also, the PABI algorithm converges very fast and after a few iterations to the final solution while preserving privacy of all independent system operators because individual variables are not shared and each system operator is informed only about a part of boundary variables of its connected networks.

References

[1] Zargar RHM, Yaghmaee MH. Energy exchange cooperative model in SDN-based interconnected multi-microgrids. Sustain Energy Grids Networks 2021;27:100491.
[2] Karimi H, Jadid S. Two-stage economic, reliability, and environmental scheduling of multi-microgrid systems and fair cost allocation. Sustain Energy Grids Networks 2021;28:100546.
[3] Baghbanzadeh D, Salehi J, Gazijahani FS, Shafie-khah M, Catalao JP. Resilience improvement of multi-microgrid distribution networks using distributed generation. Sustain Energy Grids Networks 2021:100503.
[4] Mohamed MA, Hajjiah A, Alnowibet KA, Alrasheedi AF, Awwad EM, Muyeen S. A secured advanced management architecture in peer-to-peer energy trading for multi-microgrid in the stochastic environment. IEEE Access 2021;9:92083–100.
[5] Younesi A, Shayeghi H, Safari A, Siano P. Assessing the resilience of multi microgrid based widespread power systems against natural disasters using Monte Carlo Simulation. Energy 2020;207:118220.
[6] Hakimi SM, Hasankhani A, Shafie-khah M, Catalão JP. Stochastic planning of a multi-microgrid considering integration of renewable energy resources and real-time electricity market. Appl Energy 2021;298:117215.

[7] Qu Z, Chen J, Peng K, Zhao Y, Rong Z, Zhang M. Enhancing stochastic multi-microgrid operational flexibility with mobile energy storage system and power transaction. Sustain Cities Soc 2021;71:102962.
[8] Ahmadi SE, Rezaei N. A new isolated renewable based multi microgrid optimal energy management system considering uncertainty and demand response. Int J Electr Power Energy Syst 2020;118:105760.
[9] Karimi H, Jadid S. Optimal energy management for multi-microgrid considering demand response programs: a stochastic multi-objective framework. Energy 2020;195:116992.
[10] Samuel O, Javaid N, Khalid A, Khan WZ, Aalsalem MY, Afzal MK, et al. Towards real-time energy management of multi-microgrid using a deep convolution neural network and cooperative game approach. IEEE Access 2020;8:161377–95.
[11] Cao Y, Li D, Zhang Y, Tang Q, Khodaei A, Zhang H, et al. Optimal energy management for multi-microgrid under a transactive energy framework with distributionally robust optimization. IEEE Trans Smart Grid 2021.
[12] Karimi H, Bahmani R, Jadid S, Makui A. Dynamic transactive energy in multi-microgrid systems considering independence performance index: a multi-objective optimization framework. Int J Electr Power Energy Syst 2021;126:106563.
[13] Jia Y, Wen P, Yan Y, Huo L. Joint operation and transaction mode of rural multi microgrid and distribution network. IEEE Access 2021;9:14409–21.
[14] Karimi H, Jadid S. Modeling of transactive energy in multi-microgrid systems by hybrid of competitive-cooperative games. Electr Pow Syst Res 2021;201:107546.
[15] Rajaei A, Fattaheian-Dehkordi S, Fotuhi-Firuzabad M, Moeini-Aghtaie M. Decentralized transactive energy management of multi-microgrid distribution systems based on ADMM. Int J Electr Power Energy Syst 2021;132:107126.
[16] Mazidi M, Rezaei N, Ardakani FJ, Mohiti M, Guerrero JM. A hierarchical energy management system for islanded multi-microgrid clusters considering frequency security constraints. Int J Electr Power Energy Syst 2020;121:106134.
[17] Rashidi R, Hatami A, Abedini M. Multi-microgrid energy management through tertiary-level control: Structure and case study. Sustainable Energy Technol Assess 2021;47:101395.
[18] Dawoud NM, Megahed TF, Kaddah SS. Enhancing the performance of multi-microgrid with high penetration of renewable energy using modified droop control. Electr Pow Syst Res 2021;201:107538.
[19] Brahmia I, Wang J, Xu H, Wang H, Turci LDO. Robust data predictive control framework for smart multi-microgrid energy dispatch considering electricity market uncertainty. IEEE Access 2021;9:32390–404.
[20] Li Q, Li R, Pu Y, Li S, Sun C, Chen W. Coordinated control of electric-hydrogen hybrid energy storage for multi-microgrid with fuel cell/electrolyzer/PV/battery. J Storage Mater 2021;42:103110.
[21] Nejabatkhah F, Li YW. Overview of power management strategies of hybrid AC/DC microgrid. IEEE Trans Power Electron 2014;30:7072–89.
[22] Zhou Q, Shahidehpour M, Li Z, Che L, Alabdulwahab A, Abusorrah A. Compartmentalization strategy for the optimal economic operation of a hybrid ac/dc microgrid. IEEE Trans Power Syst 2019;35:1294–304.
[23] Maulik A, Das D. Optimal power dispatch considering load and renewable generation uncertainties in an AC–DC hybrid microgrid. IET Gener Transm Distrib 2019;13:1164–76.
[24] Xia Y, Wei W, Yu M, Peng Y, Tang J. Decentralized multi-time scale power control for a hybrid AC/DC microgrid with multiple subgrids. IEEE Trans Power Electron 2017;33:4061–72.
[25] Wu P, Huang W, Tai N, Liang S. A novel design of architecture and control for multiple microgrids with hybrid AC/DC connection. Appl Energy 2018;210:1002–16.
[26] Bhat Nempu P, Jayalakshmi N. Coordinated power management of the subgrids in a hybrid AC–DC microgrid with multiple renewable sources. IETE J Res 2020:1–11.
[27] Xia Y, Wei W, Yu M, Wang X, Peng Y. Power management for a hybrid AC/DC microgrid with multiple subgrids. IEEE Trans Power Electron 2017;33:3520–33.
[28] Rousis AO, Konstantelos I, Strbac G. A planning model for a hybrid AC–DC microgrid using a novel GA/AC OPF algorithm. IEEE Trans Power Syst 2019;35:227–37.
[29] Morgan MY, Shaaban M, Sindi H, Zeineldin H. A holomorphic embedding power flow algorithm for islanded hybrid AC/DC microgrids. IEEE Trans Smart Grid 2022.
[30] D. Pullaguram, R. Madani, T. Altun, A. Davoudi, Optimal power flow in AC/DC microgrids with enhanced interlinking converter modeling, IEEE J Emerg Select Top Industrial Electronics, 2022.
[31] Du Y, Lu X, Chen B, Lin F. Resiliency augmented hybrid AC and DC distribution systems with inverter-dominated dynamic microgrids. IEEE Trans Smart Grid 2022.
[32] Muhtadi A, Pandit D, Nguyen N, Mitra J. Distributed energy resources based microgrid: review of architecture, control, and reliability. IEEE Trans Ind Appl 2021.
[33] Du Y, Wang Z, Liu G, Chen X, Yuan H, Wei Y, et al. A cooperative game approach for coordinating multi-microgrid operation within distribution systems. Appl Energy 2018;222:383–95.
[34] Fu Y, Zhang Z, Li Z, Mi Y. Energy management for hybrid AC/DC distribution system with microgrid clusters using non-cooperative game theory and robust optimization. IEEE Trans Smart Grid 2019;11:1510–25.
[35] Zhang Y, Ai Q, Wang H, Li Z, Huang K. Bi-level distributed day-ahead schedule for islanded multi-microgrids in a carbon trading market. Electr Pow Syst Res 2020;186:106412.
[36] Zhang Z, Wang Z, Wang H, Zhang H, Yang W, Cao R. Research on Bi-level optimized operation strategy of microgrid cluster based on IABC algorithm. IEEE Access 2021;9:15520–9.
[37] Arefifar SA, Ordonez M, Mohamed Y-A-R-I. Energy management in multi-microgrid systems—development and assessment. IEEE Trans Power Syst 2016;32:910–22.
[38] Zhao B, Wang X, Lin D, Calvin MM, Morgan JC, Qin R, et al. Energy management of multiple microgrids based on a system of systems architecture. IEEE Trans Power Syst 2018;33:6410–21.
[39] Xu Y, Zhang J, Wang P, Lu M. Research on the Bi-level optimization model of distribution network based on distributed cooperative control. IEEE Access 2021;9:11798–810.
[40] Arpanahi MK, Nateghi A, Shafie-khah M. A coordinated decentralized loss minimization scheme for hybrid AC/DC distribution system with multiple microgrids. Int Conf Smart Energy Syst Technol (SEST) 2021;2021:1–6.
[41] Matsumoto A, Szidarovszky F. Game theory and its applications. Springer; 2016.
[42] Boyd S, Boyd SP, Vandenberghe L. Convex optimization. Cambridge University Press; 2004.
[43] J. Savier, D. Das, Impact of network reconfiguration on loss allocation of radial distribution systems, IEEE Transactions on Power Delivery, vol. 22, pp. 2473-2480.
[44] Beerten J, Cole S, Belmans R. Generalized steady-state VSC MTDC model for sequential AC/DC power flow algorithms. IEEE Trans Power Syst 2012;27(2):821–9.